

POLITECNICO DI TORINO

DIPARTIMENTO DI INGEGNERIA MECCANICA E
AEROSPAZIALE (DIMEAS)

Master's Degree in Biomedical Engineering

Master's Degree Thesis

**Average Threshold Crossing
Validation for Functional Electrical
Stimulation Applied to Surface
ElectroMyoGraphic Signals**



Supervisors:

Prof. Danilo DEMARCHI

Dr. Paolo MOTTO ROS

Candidate

Sofia CECCHINI

matricola: 230824

TORINO, JULY 2018

Abstract

Average Threshold Crossing (ATC) technique consists of the generation of an event every time a specific signal exceeds a certain threshold. As far as the surface ElectroMyoGraphic (sEMG) signal is concerned, the ATC parameter is proved to be highly correlated to the muscle contraction force. This project thesis proposes the improvement and the validation of a low power system based on the application of the ATC technique to the sEMG signal, in order to perform the Functional Electrical Stimulation (FES). FES is a therapy consisting of a series of low amplitude current pulses commonly employed to restore motor functions in the affected limbs of spinal chord injury and stroke patients. The system allows the reproduction of a specific movement performed by a controller subject from whom the sEMG signal is acquired, in the affected limb of the subject under control, by means of FES. In order to assess the validation of the system, two articular goniometers were realised and integrated in the whole system to track the joint angles involved with the aim of measuring the similarity between the two movements.

The system consists of three main parts: an *acquisition* unit, an *elaboration* unit and finally an *actuation* unit.

An acquisition board with four analog channels acquires and processes the sEMG and counts the number of TC events generated. Afterwards, the information related to the muscle contraction is sent to the Matlab[®] workstation through Bluetooth Low Energy communication, where the FES therapy is elaborated and sent to the stimulator and the joint angles of the controller and controlee movements are acquired simultaneously to the acquisition and stimulation processes. Experimental tests have been conducted performing 12 tests on 19 healthy subjects involving four movements: elbow flexion, elbow extension, ankle dorsi-flexion, ankle plantar flexion.

The obtained results showed that the movement of the subject under control can be mimicked with high fidelity compared to that of the controller.

Summary

The aim of this thesis project is the improvement and the validation of a low power system based on event-driven technique for the control of Functional Electrical Stimulation (FES). It has been developed for rehabilitative purposes concerning hemiplegic, para- and tetraplegic subjects. In future developments, it will be possibly employed in *active rehabilitation* procedures which consist of the performance of a specific movement by the therapist and the subsequent reproduction of the same movement by the patient. Alternatively *self-administered rehabilitation* procedure can be conducted, according to which the patient can autonomously perform the rehabilitative exercises in the affected limb by the execution of the movement in the healthy limb. The latter solution could be exploited by hemiplegic patients. Following this general idea, this system allows the reproduction of a movement performed by a controller subject by the controlee subject. The system validation is conducted acquiring simultaneously with the stimulation process the angle trends of the selected joint for the movement involved for both therapist and patient. A good performance of the system corresponds to an high correlation between the two angle trends. This means that the controlee movement is greatly similar to that of the controller.

The system functioning is based on the surface ElectroMyoGraphic (sEMG) signal acquisition from the therapist or the healthy limb of the patient, the subsequent data transmission to the computer workstation and finally the elaboration of the relative FES therapy delivered to the affected limb of the patient.

The thesis is divided into six chapters. In the Introduction chapter fundamental notions about the skeletal muscle physiology and the contraction mechanism are reported in section 1.1. Then a wide overview regarding sEMG is provided in section 1.2: the main signal characteristics together with the acquisition modality are described. Section 1.3 provides the description of the Average threshold Crossing (ATC) parameter and its main advantages compared to the traditional techniques. Then Functional Electrical Stimulation is described in section 1.4 and finally a general overview regarding the definition of the Range Of Motion (ROM), the articular goniometers used to measure it is given in section 1.5 together with a detailed explanation of the functioning principle of the encoder, which is used as

the angle sensor in this thesis project.

The second chapter describes in the first two sections the State of Art of the sEMG acquisition systems (section 2.1), the Average Threshold Crossing technique description when applied to the sEMG signal in particular (section 2.2). Section 2.3 gives an overview of the State of Art of the FES-sEMG system available and finally a review of the advantages and drawbacks of the different types of absolute encoders.

The third chapter shows the system architecture as far as the the acquisition unit, data transmission process and data elaboration are concerned (section 3.1). Section 3.2 is thus reserved for the description of the different steps necessary for the articular goniometer realisation which start from the sensor illustration to the angle data acquisition procedure and end with the realisation of a proper case. Afterwards the Matlab[®] Graphical User Interface is described with all its functionalities (section 3.3) that allows the choice and the performance of a certain action by the user. Finally in section 3.4 an overview of the Matlab[®] and Simulink[®] code is provided.

Afterwards, the acquisition protocol is described in chapter four. Its sections illustrates the acquisition and stimulating electrodes characteristics and positioning, the movements analysed and the calibration phase performed before the start of the real acquisition procedure.

In chapter five the analysis of the obtained data is explained. In section 5.1 the parameters extracted from the angle signals and stimulation trend are enumerated while the following section presents the results achieved.

Finally chapter six briefly summerise the work done and the obtained results, introducing also some future developments.

Contents

| | |
|--|----|
| Summary | II |
| 1 Introduction | 1 |
| 1.1 The skeletal muscle | 1 |
| 1.1.1 Skeletal muscle structure | 1 |
| 1.1.2 Contraction mechanism | 3 |
| 1.2 Surface electromyography (sEMG) | 6 |
| 1.2.1 EMG Signal Morphology | 7 |
| 1.2.2 EMG Acquisition Techniques | 8 |
| 1.2.3 sEMG Acquisition Electrodes | 8 |
| 1.2.4 Noise Sources | 11 |
| 1.2.5 EMG Feature Extraction | 12 |
| 1.3 Average Threshold Crossing (ATC) | 15 |
| 1.4 Functional Electrical Stimulation (FES) | 16 |
| 1.4.1 FES Parameters | 16 |
| 1.5 Range Of Motion (ROM) | 17 |
| 1.5.1 Articular Goniometers | 18 |
| 1.5.2 Rotary Encoder | 18 |
| 2 State of Art | 21 |
| 2.1 sEMG Acquisition Systems | 21 |
| 2.2 ATC technique applied to sEMG | 22 |
| 2.3 FES-sEMG systems | 23 |
| 2.4 Features of absolute encoders and their role in human joint angles analysis | 26 |
| 3 System Architecture | 27 |
| 3.1 System Architecture Description | 28 |
| 3.1.1 Acquisition Board and Data Transmission | 29 |
| 3.1.2 Data Elaboration and Stimulation | 30 |

| | | |
|----------|---|-----------|
| 3.1.3 | Actuation | 33 |
| 3.2 | Articular Electrogoniometer Realisation | 35 |
| 3.2.1 | AMT20 Absolute Encoder | 35 |
| 3.2.2 | Angle Data Acquisition | 37 |
| 3.2.3 | Angle Data Elaboration | 38 |
| 3.2.4 | Articular Goniometer Case | 38 |
| 3.3 | Software control and elaboration of the operations | 41 |
| 3.4 | Matlab Graphical User Interface (GUI) | 42 |
| 3.4.1 | FES setup GUI | 44 |
| 3.5 | Matlab [®] and Simulink [®] code overview | 46 |
| 3.6 | Definition of the stimuli sequence from the TC data | 50 |
| 4 | Experimental Acquisitions | 53 |
| 4.1 | Acquisition Protocol Description | 53 |
| 4.1.1 | Acquisition Electrodes | 53 |
| 4.1.2 | Stimulating Electrodes | 55 |
| 4.1.3 | Movements Analysed | 55 |
| 4.1.4 | Calibration Phase | 59 |
| 5 | Data Analysis | 61 |
| 5.1 | Parameters extraction | 61 |
| 5.2 | Fatigue Analysis | 65 |
| 5.3 | Results | 66 |
| 5.3.1 | System Time Performances | 70 |
| 6 | Conclusion | 73 |
| 6.1 | Results and future Developments | 74 |
| | Bibliography | 77 |

List of Tables

| | | |
|-----|---|----|
| 3.1 | Rehastim Stimulator [®] and Dongle CC2540 serial COM port configurations. | 32 |
| 3.2 | Technical specification of the RehaStim2 stimulator [35]. | 33 |
| 3.3 | Arduino serial COM port configuration. | 38 |
| 3.4 | FES parameters initially set in the GUI by the user. | 45 |
| 4.1 | Kendall [™] Electrodes Characteristics. | 54 |
| 4.2 | Order of the sequence of session and repetitions in the chosen protocol. Each repetition consists of a sequence of ten consecutive movements. The repetition of each of the four selected movements has a different order through the three sessions. | 56 |
| 4.3 | Stimulation parameters chosen for every movement performed. | 56 |
| 5.1 | Parameters analysis within each session | 65 |
| 5.2 | Final results | 66 |

List of Figures

| | | |
|------|--|----|
| 1.1 | Skeletal muscle structure [4]. | 2 |
| 1.2 | Sarcomere structure [5]. | 3 |
| 1.3 | Skeletal muscle action potential [6]. The resting potential (-70 mV) progressively rises until reaching the threshold which triggers the action potential, with a maximum potential value of 30 mV. At this point a depolarisation phase followed by a repolarisation phase occur, until the original potential is restored. | 4 |
| 1.4 | Types of contractions: (1.4a Muscles contract but do not shorten, (1.4b) Muscles contract and shorten to lift the weight, (1.4c) Muscles contract but lengthen to control the lowering of the weight [36]. | 5 |
| 1.5 | Force of contraction exerted in response of a single stimulus (1.5a) or multiple stimuli resulting in summation (1.5b) or tetanus (1.5c) if the stimulation frequency is high enough [7]. | 6 |
| 1.6 | Electromyography decomposition in order to individually define each Motor Unit Action Potential [8]. | 7 |
| 1.7 | Example of EMG signal and its frequency spectrum [17]. | 8 |
| 1.8 | Electrode-electrolyte interface reactions [36]. | 9 |
| 1.9 | Electrode-electrolyte equivalent circuit. [17]. | 10 |
| 1.10 | sEMG Recording Configurations [37]. | 10 |
| 1.11 | Average Threshold Crossing (ATC) technique [20]. | 15 |
| 1.12 | FES parameters description [25]. | 17 |
| 1.13 | Example of elbow joint ROM [26]. | 18 |
| 1.14 | Encoder functioning. If A leads B, signal A shows a rising edge before signal B and the disk is rotating in a counterclockwise direction, otherwise the direction is clockwise. [27]. | 19 |
| 1.15 | Capacitive Encoder. [27]. | 20 |
| 2.1 | EMG Conditioning Stages. | 22 |

| | | |
|------|--|----|
| 2.2 | sEMG controlled FES system [44]. The electromyographic signal acquired triggers the functional stimulation after being processed and contributes to the FES parameters adjustment together with the joint angle signal. | 24 |
| 2.3 | CCFES description [45]. As it can be seen in 2.3b, the EMG signal from the non-paretic hand (Muscle1) is acquired, thresholded and used to set the proper FES parameters for the affected limb (Muscle2). | 24 |
| 2.4 | Direct rehabilitation method based on the use of FES and EMG [46]. The EMG signal is acquired from the therapist, capable of an ideal contraction pattern, and subsequently evaluated to elaborate the right stimulation pattern for the patient. Eventually, information on inappropriate EMG patterns are transmitted from the patient to the therapist. | 25 |
| 3.1 | General scheme of the system functioning | 28 |
| 3.2 | General work-flow of the system functioning | 28 |
| 3.3 | The PCB used to acquire the sEMG signals [39]. It includes a power supply unit, a central digital interface and four possible analog front-end channel units | 29 |
| 3.4 | RehaStim2 [®] Simulink [®] interface. | 31 |
| 3.5 | Characteristics of a current pulse delivered by RehaStim2 stimulator [35]. | 33 |
| 3.6 | Example of a RehaStim2 [®] stimuli pattern [35]. Channels 1, 2 from Module A and 5, 7 from Module B are selected and set with the same width and amplitude. The channels 1 and 2 mode is the doublet characterised by an inter pulse interval. The stimulation pattern is repeated after a main stimulation interval. | 34 |
| 3.7 | AMT20 absolute encoder. [27]. | 36 |
| 3.8 | SPI Master-Slave architecture [32]. | 36 |
| 3.9 | SPI timing diagram [33]. | 37 |
| 3.10 | Encoder CAD model created with Solidworks [®] | 39 |
| 3.11 | Electrogoniometer final implementation. | 40 |
| 3.12 | Actions and roles played by Matlab [®] and Simulink [®] | 41 |
| 3.13 | Main Graphical User Interface (GUI) created in Matlab [®] environment. | 42 |
| 3.14 | Graphical User Interface (GUI) used to set the proper stimulation and acquisition parameters. | 44 |
| 3.15 | Simulink [®] stimulation top level model | 47 |
| 3.16 | Simulink [®] stimulation model blocks content | 48 |
| 3.17 | Flowchart of the actions performed once the stimulation is started. | 49 |
| 3.18 | Setting of the acquisition-stimulation relation parameters during the calibration phase | 50 |
| 3.19 | Flowchart of the ATC parameter-current amplitude definition during the acquisition-stimulation process. | 52 |
| 4.1 | Covidien [™] Kendall [™] electrode | 54 |

| | | |
|------|---|----|
| 4.2 | Stimulating Electrodes produced by HASOMED RehaTrode® | 55 |
| 4.3 | Elbow flexion (Biceps brachii) | 57 |
| 4.4 | Elbow extension (Triceps brachii muscle) | 57 |
| 4.5 | Ankle dorsi-flexion (Tibialis anterior) | 58 |
| 4.6 | Ankle plantar-flexion (Gastrocnemius, lateral head) | 58 |
| 5.1 | Angle features extracted | 63 |
| 5.2 | Data Analysis GUI | 64 |
| 5.3 | Boxplots of the first four parameters for elbow flexion | 68 |
| 5.4 | Boxplots of the first four parameters for elbow extension | 68 |
| 5.5 | Boxplots of the first four parameters for ankle dorsi-flexion | 69 |
| 5.6 | Boxplots of the first four parameters for ankle plantar-flexion | 69 |
| 5.7 | Boxplots of the timing parameters for elbow flexion | 71 |
| 5.8 | Boxplots of the timing parameters for elbow extension | 71 |
| 5.9 | Boxplots of the timing parameters for ankle dorsi-flexion | 72 |
| 5.10 | Boxplots of the timing parameters for ankle plantar-flexion | 72 |

Chapter 1

Introduction

1.1 The skeletal muscle

Muscle tissue is a specialized tissue which has the ability to contract. It is divided into three types: skeletal muscle, myocardium and smooth muscle. Smooth and cardiac muscle contraction is involuntary and could be activated by the central, peripheral or endocrine nervous system. On the contrary, the skeletal muscle is contracted voluntarily with conscious intervention under the control of the somatic nervous system.

Skeletal muscle covers the vast majority of our muscle tissue and the 40% of the body weight. Its main function is to convert chemical energy into mechanical energy generating force and power, producing body movement and maintaining posture [1]. It has also an important metabolic function, acting as a repository for relevant substrates such as amino acids and carbohydrates. Its composition includes water (75%), protein (20%), and other substances including inorganic salts, minerals, fat, and carbohydrates (5%). In general, muscle mass is highly susceptible to factors such as nutritional status, hormonal balance, physical activity/exercise, and injury or disease, among others [2].

1.1.1 Skeletal muscle structure

Skeletal muscle is composed of several fascicles of muscle fibers covered by connective tissue, the epimysium, which is connected to the tendon, the structure made of fibrous connective tissue that connects muscle to bone and whose main function is to transmit forces during movements. Layers of connective tissue, fundamental for the muscle vascularisation and innervation, surround every fascicle (perimysium) and separate each muscle fiber inside the fascicles (endomysium), as it can be seen in figure 1.1. The plasma membrane sarcolemma covers the striated

muscle fibers, which are mostly composed of myofibrils, contractile fibres made up of thick (myosin) and thin (actine) myofilaments parallel to the length of the cylindrical fibre. The thick filaments are composed of myosin, and the thin filaments are predominantly actin, along with two other muscle proteins, tropomyosin and troponin. Muscular contraction is generated by the temporary bound between the two myofilaments [3].

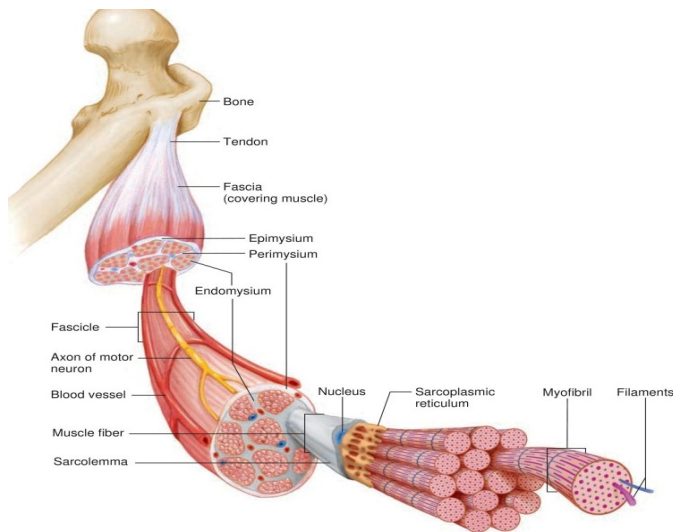


Figure 1.1: Skeletal muscle structure [4].

In the myofibril structure, sarcomeres, the fundamental contractile motor units, alternate. The sarcomere is delimited by two consecutive I bands, light regions which present only actin filaments while the dark center part (A band) is dominated by myosin partly overlapped with the thin filament (Fig. 1.2). Tension in the muscle is produced by the slide of the thin filament over the thick one and the consequent shortening of the I band and the sarcomere overall.

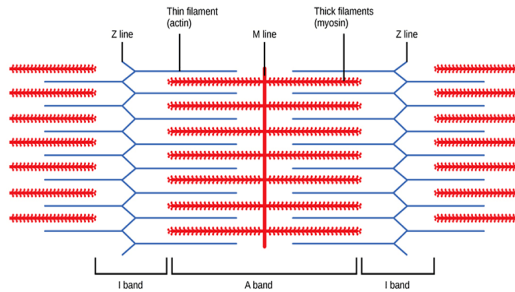


Figure 1.2: Sarcomere structure [5].

1.1.2 Contraction mechanism

Muscle Action Potential Generation and contraction

Skeletal muscles contractions are the result of a voluntary effort, which originates in the brain. The electrochemical signal related to the volition of contraction is transmitted through the nervous system to the motor neuron which innervates muscle fibers. The signal, known as action potential, is the result of the membrane potential fluctuations in excitable cells, caused by depolarisations or hyperpolarisations which occur as a result of the sodium voltage dependent gate openings and closings.

A motor neuron and the skeletal muscle fibers innervated by that motor neuron's axonal terminals, form the *motor unit*. The action potential that propagates along the motor neuron reaches the neuromuscular junction, the chemical synapse between the motor neuron and the muscle fiber, allowing the release of acetylcholine (ACh) in the cleft. Acetylcholine then binds to the ACh receptor in the sarcolemma, triggering a *muscle action potential* (AP). The shape of a typical skeletal muscle action potential is shown in figure 1.3. The contraction is possible by the presence of the *sarcoplasmic reticulum*, which has terminal cisternae that store and release Ca^{2+} ions. Transverse tubule, an invagination of the sarcolemma, conducts the muscle action potential uniformly inside the fiber, triggering the release of Ca^{2+} ions in the sarcoplasm. At this point calcium ions bind to troponin C in the actin filaments. This bound prevent the tropomyosin blocking the active site of the actine filament, allowing the slide of the thin filament over the thick one (crossbridge cycling).

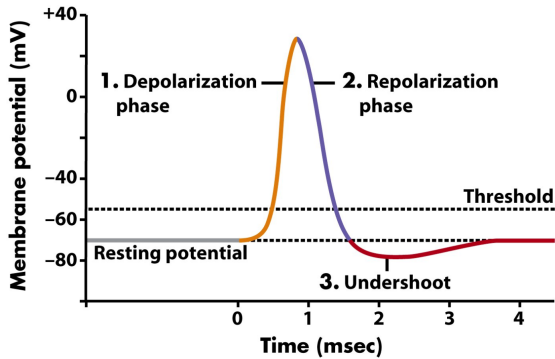


Figure 1.3: Skeletal muscle action potential [6]. The resting potential (-70 mV) progressively rises until reaching the threshold which triggers the action potential, with a maximum potential value of 30 mV. At this point a depolarisation phase followed by a repolarisation phase occur, until the original potential is restored.

Types of Contraction

Muscle contraction could be performed maintaining or changing the length of the muscle itself and may be classified according to these different behaviours.

Isotonic contraction involves the change of the muscle length resulting in a movement (dynamic contraction). It can be concentric if there is a shortening of the muscle while the tension is kept at a fixed value. This kind of contraction is elicited for example during the lift of a load, which is less than the maximum tetanic force of the muscle involved.

Eccentric contractions implies instead the lengthening of the fibers while responding to a greater opposing force compared to the maximum tension that the muscle can generate.

On the contrary, *isometric contractions* presents changes in tension and energy while the muscle length is kept constant. These conditions imply that no movement is performed and there is no change in the angle joint (static contraction). This situation generally occurs while providing force against an immovable load [7].

A visual explanation is provided in figure 1.4.

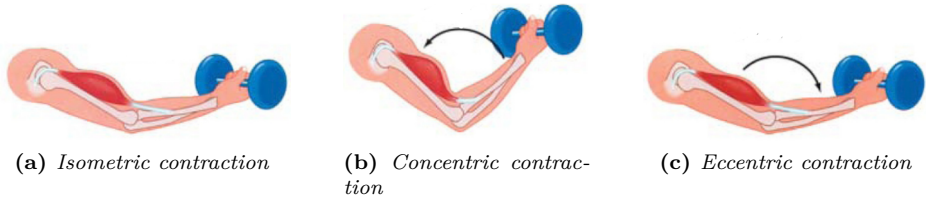


Figure 1.4: Types of contractions: (1.4a) Muscles contract but do not shorten, (1.4b) Muscles contract and shorten to lift the weight, (1.4c) Muscles contract but lengthen to control the lowering of the weight [36].

Force of contraction

A single contraction and relaxation cycle produced by a single stimulus (muscle action potential) is called *twitch* (Fig. 1.5a). The effective muscle contraction occurs after a delay from the stimulation of the muscle, due to the time requested for muscle depolarisation, calcium ions diffusion and the establishment of the cross-bridge bound. This lag time, known as *latent period*, usually takes 10 ms [9]. The contraction period, characterised by a continuous increase of the tension produced, has a duration of about 10-100ms. Afterwards, the muscle starts relaxing producing a consequent force of contraction downward trend. If a stimulus is able to trigger another muscle action potential before the complete relaxation phase of a muscle twitch, a second twitch will sum onto the first one resulting in an increase of the intensity of the overall muscle contraction.

This phenomenon called *summation*, could be achieved in two ways: frequency summation and multiple fiber summation (Fig. 1.5b). *Frequency summation* consists of increasing the frequency at which action potentials are triggered in the muscle fibers provoking the consequent rise of the force of contraction. The principle of *multiple fiber summation* is the variation of the recruitment of muscle fibers, which depends on the strength of the signal transmitted; the smallest motor units are stimulated first, as the signal becomes stronger, larger motor units that have 50 times the contractile strength as the smaller ones, are excited increasing the force of muscle contraction. Nevertheless, both events typically occur concurrently, even if the latter is predominant at low forces while the first dominates at greater forces and during fast contractions.

If the frequency of stimulation is such that the muscle does not have enough time to relax, the force of contraction reaches its maximum value and remains constant. This condition is known as *tetanus*, as it is shown in figure 1.5c.

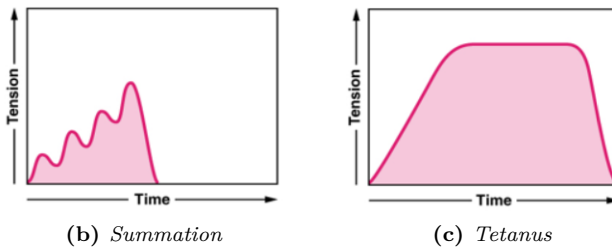
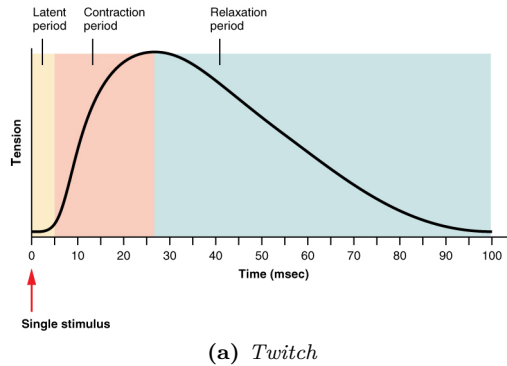


Figure 1.5: Force of contraction exerted in response of a single stimulus (1.5a) or multiple stimuli resulting in summation (1.5b) or tetanus (1.5c) if the stimulation frequency is high enough [7].

1.2 Surface electromyography (sEMG)

Each motor neuron can be located in the brain stem or the spinal cord, with his axons that exit through the ventral root if the neuron is located in the spinal chord, or through a cranial nerve if it origins in the brain stem. The axons projects in a peripheral nerve to its target muscle. As it has been previously stated, each motor neuron innervates with his axons and dentrites several muscle fibers, forming a complex known as *motor unit*. The action potential of the motor neuron leads to the propagation of action potentials in all the muscle fibers belonging to the motor unit with a speed, defined as *conduction velocity*, that depends on the fibers diameter, skin temperature and extracellular concentrations of metabolites.

The electromyographic (EMG) signal is the summation of the action potentials originating from many motor units (MUs) showing the muscle response to neural stimulation. It provides muscle’s anatomical and physiological information, fundamental in clinical diagnosis and biomedical applications especially rehabilitation of motor disability. It appears random in nature and is generally modeled as a filtered impulse process where the Motor Unit Action Potential (MUAP) is the

filter and the impulse process stands for the neuron pulses, often modeled as a Poisson process. In order to obtain individually the motor unit action potentials, it is necessary the decomposition of the EMG signal, as explained in figure 1.6.

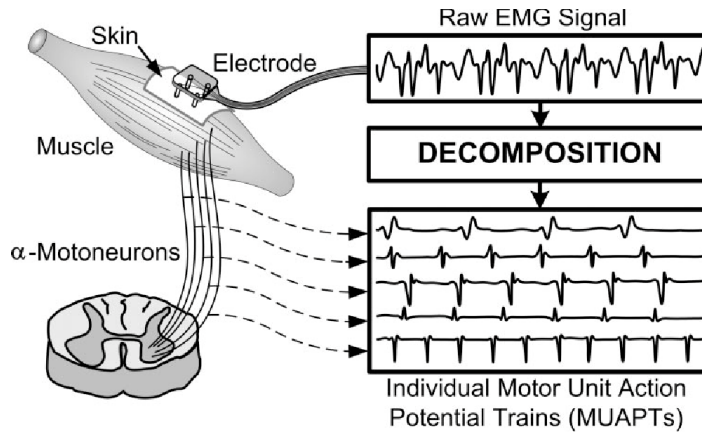


Figure 1.6: Electromyography decomposition in order to individually define each Motor Unit Action Potential [8].

1.2.1 EMG Signal Morphology

EMG signal amplitude is stochastic in nature and varies from tens of μV to few mV while its bandwidth is defined between 20 Hz and 500 Hz [13], even if the main frequency contribution ranges from 50 Hz to 150 Hz (Fig. 1.7).

In order to perform a satisfying acquisition, the *signal to noise ratio* and the *distortion of the signal* should be taken in consideration. The first is defined as the ratio of the energy in the signal of interest to the energy in the noise signal, such as the unwanted electrical signals which affect the EMG signal information, while the distortion of the signal consists in the altered correspondence of the relative contribution of the frequency components in the EMG signal [17].

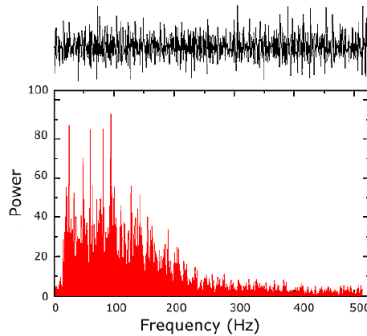


Figure 1.7: Example of EMG signal and its frequency spectrum [17].

1.2.2 EMG Acquisition Techniques

The signal could be acquired through needle or wire electrodes inserted directly into the muscle (*intramuscular electromyography*) or using surface electrodes placed on the patient skin (*surface electromyography*). The latter, compared to the intramuscular technique, has a large pick-up area, but accurately records the activity of superficial muscles that are less than 1.8 cm deep [12]. It is greatly affected by cross-talk as it partly records the activity of the muscles nearby together with the muscles of interest. Therefore, it is considered a less reliable technique compared to the use of intramuscular needles. Nevertheless it is totally non-invasive, painless and it could be performed easily even by non-medical staff.

1.2.3 sEMG Acquisition Electrodes

Biopotential electrodes

Biopotential electrodes are sensors that convert ionic conduction flowing in our body to electronic conduction, obtaining biopotential signals which have important clinical and diagnostic information.

Electrodes are obviously made of conductive material, such as metal atoms. When it is in contact with an electrolyte solution (a conductive solution containing water, anions and cations composed of the same electrode material), two phenomena might occur:

- *Oxidation*: when a metal atom in the electrode lose electrons which remain in the electrode itself, while its cation is discharged into the electrolyte (current flow from electrode to electrolyte, fig. 1.8a).
- *Reduction*: when a cation in the solution combines with electrons in the electrode (current flow from electrolyte to electrode, fig. 1.8b).

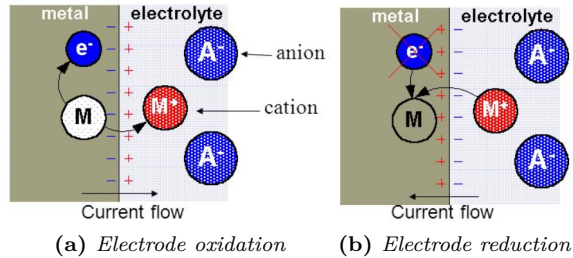


Figure 1.8: Electrode-electrolyte interface reactions [36].

As a result, two parallel layers of ions having opposite charge are formed, producing a potential difference (*half-cell potential*), which depends on the metal, ions concentration in the electrolyte and temperature. The half-cell potential is measured using the hydrogen electrode as the having the reference potential, which is therefore set to zero (*standard half-cell potential*).

According to the phenomena occurring in the electrode-electrolyte interface, the electrodes can be ideally categorised in:

- *Perfectly Polarizable*: when applying a current, the electrode acts as a capacitor since there is no actual passing of charges within the interface (electrodes made of noble metals, such as platinum).
- *Perfectly Non-Polarizable*: charges freely cross the interface (for example silver/silver chloride electrodes).

Electrode Equivalent Circuit

Figure 1.9 shows the resulting equivalent circuit for the electrode-electrolyte interface. E_{hc} is the half-cell potential, R_d the resistance representing the current flowing across the interface, C_d the capacitance associated with the double layer of opposite charges and R_s the resistance of the electrode lead wire. If the electrode is polarizable, the capacitive component will prevail to the resistive one in parallel (stimulating electrode), while if it is non-polarizable the opposite phenomenon will occur (acquisition electrode).

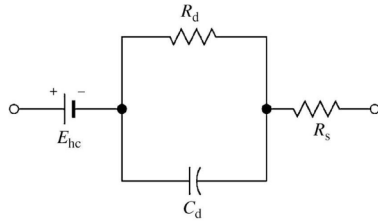


Figure 1.9: Electrode-electrolyte equivalent circuit. [17].

sEMG Acquisition system configuration

As far as the acquisition process is concerned, two are the main sEMG configurations: *monopolar* (Fig. 1.10a) and *bipolar* (Fig. 1.10b). The first measures the voltage difference between the electrode placed over the belly of the muscle and the reference electrode placed in an electrically neutral area. In bipolar configuration, the biosignal is determined as the difference of two electrode potentials placed on the muscle belly, each one calculated respect to the reference electrode.

The differential amplifier used in the bipolar configuration, has the great advantage to suppress the common noise signals before amplifying the difference. Therefore, it is the most common used configuration.

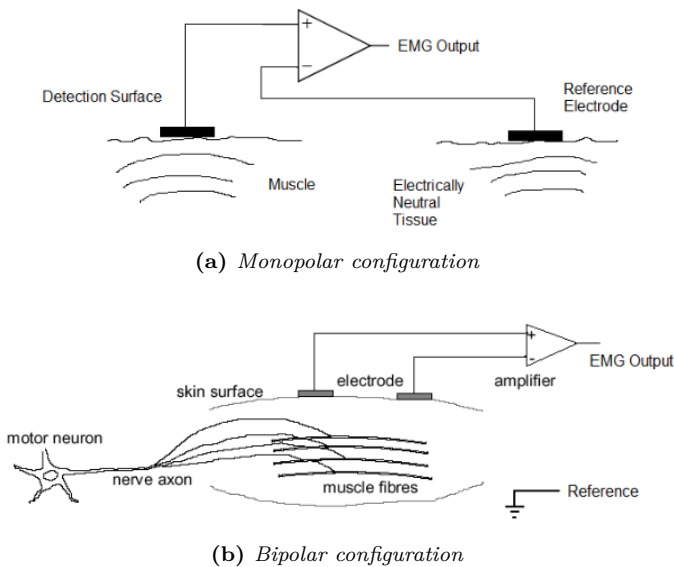


Figure 1.10: sEMG Recording Configurations [37].

1.2.4 Noise Sources

Surface EMG signal is deeply affected by noise, which could be due to several factors [14]:

Inherent noise in the electrode. It is the noise generated by the electronic equipment, whose bandwidth range from 0 Hz to thousand Hz. Using high quality instruments and intelligent circuit design could help in decreasing the influence of inherent noise. The choice of the electrodes materials and size could also be relevant. An acceptable compromise must be chosen between large electrodes, which provide a lower impedance and consequently a better signal quality and smaller electrodes which have higher impedance, lower signal-to-noise ratio but higher muscle selectivity.

Movement artifact. The relative movement between the surface electrodes and the skin during the muscle contraction, generates motion artifacts, whose frequency range from 1 Hz to 10 Hz and whose amplitude is comparable to that of sEMG signal. In order to reduce the noise produced by this type of event, a conductive layer must be used between the skin and the electrode-electrolyte interface. A second motion artifact occurs when there is a difference between the layers of the skin. In this case scratching the skin and consequently reducing the skin impedance, attenuate the magnitude of the artifact.

Electromagnetic noise. Electromagnetic radiations coming from the environment produce ambient noise, which has an amplitude comparable and sometimes even three times greater than the sEMG. This kind of noise is impossible to eliminate since the human body himself continuously generates electromagnetic radiations. Nevertheless, the main contribution is made by radiations at 60 Hz (or 50 Hz) from power sources (*Power-Line Interference, PLI*). Stray currents and electrode impedances differences generally produce the noise. Therefore, if the frequency of the noise is found within the bandwidth of the signal of interest, proper filters should be applied during a post-processing analysis.

Cross Talk. It is defined as the electrical activity originating from active neighbouring muscles which affects the quality of the sEMG signal of muscle of interest. Its amplitude is about the 16% of that of a stimulated crosstalk muscle signal [15]. The influence of cross talk noise depends on factors such as *electrode size*, *inter-electrode spacing* and the *location of the sensor*. The latter could be optimised placing the sensor in the middle of the muscle belly in the axis direction of the underlying muscular fibers. Electrodes with smaller active area (and housings) permit a smaller inter-electrode distance and therefore, a higher selectivity [16]. It is then clear that the recording of the activity of broader and larger muscles requires electrodes with larger detection area and greater inter-electrode spacing. Nevertheless, increasing inter-electrodes distance results in the rise of the amplitude of both target signal and cross talk signal. Thus, the choice of spacing and size

depends on the muscle dimension and location and they both should be adjusted in order to minimise the cross talk signal but still have a acceptable electromyographic signal amplitude. Cross talk also depends on physiological aspects; it rises as the fat thickness increases.

Internal noise. The conductivity and permittivity of both muscle and skin are responsible of capacitive effects, causing internal noise during sEMG acquisition. Anatomical features such as the quantity and thickness of tissue between the active muscles and the electrodes, affect surface electromyographic signal amplitude; as the subcutaneous layer increases, the amplitude of the signal detected decreases. The underlined problem could be partly solved using high pass spatial filters.

Inherent instability of the signal. The stochastic nature of the firing rate of the motor units affect the frequency components of the EMG signal between 0 and 20 Hz, which are thus unstable and must be removed from the signal.

Electrocardiographic Artifacts. Cardiac activity is the source of one of the predominant noise for the surface electromyographic signal, especially during trunk muscle and shoulder girdle electromyography. This noise component might be reduced using common-mode rejection at the recording site and through the correct placement of bipolar electrodes possibly in the direction of the heart axis. The removal of this artifact is challenging due to their similar characteristics (they are both non-stationary) and the overlap of the bandwidths of the two signals. An high pass filter at 100 Hz could be the solution for the removal of the ECG artifact, even if it affects the sEMG frequency spectrum.

1.2.5 EMG Feature Extraction

Surface electromyography signal is analysed in the field of clinical diagnosis and biomedics to obtain information about time or intensity of superficial muscle activation, in order to understand body's behaviors under normal or pathological conditions. The data extracted could be referred to the time or frequency domain; in the latter case the features are inferred from the power spectrum of the signal, obtained performing the Fast Fourier Transform (FFT) [18].

Time Domain Features

Integrated EMG. Integrated EMG (IEMG) is the sum of sEMG signal amplitude absolute values. It is representative of the muscle contraction magnitude and it is expressed using the following formula:

$$IEMG = \sum_{n=1}^N |x_n|$$

Where N and x_n stands respectively for the number of the signal samples and the generic amplitude signal sample.

Mean Absolute Value. Mean Absolute Value (MAV), known also as Average Rectified Value (AVG), is defined as the average of the rectified sEMG signal:

$$MAV = \frac{1}{N} \sum_{n=1}^N |x_n|$$

It is a measure of muscle contraction force.

Root Mean Square. Root mean Square (RMS) is calculated as:

$$RMS = \sqrt{\frac{1}{N} \sum_{n=1}^N |x_n^2|}$$

Standard deviation of sEMG. Standard deviation (STD) is a measure of the dispersion of the data acquired relative to the mean value:

$$STD = \sqrt{\frac{1}{N-1} \sum_{n=1}^N |x_n^2|}$$

Therefore, it must be as low as possible.

Variance of EMG. Variance of EMG (VAR) is defined as:

$$VAR = \frac{1}{N-1} \sum_{n=1}^N |x_n|^2$$

Waveform Length. Waveform Length (WL) is the cumulative length of waveform over the sEMG segment expressed as:

$$WL = \sum_{n=1}^N |x_{n+1} - x_n|$$

Zero Crossing. Zero Crossing (ZC) is the tracking of the number of times the signal crosses the zero threshold and it is calculated following these expressions:

$$f_k = \begin{cases} 1, & x_k x_{k+1} < 0 \\ 0, & \text{otherwise} \end{cases}$$

$$ZC = \sum_{k=1}^{N-1} f_k$$

Willison Amplitude. Willison Amplitude (WAMP) is defined as the number of times the difference between the amplitude of two consecutive EMG signal samples exceeds a determinate threshold (x_{th}), set at 10 mV:

$$f(x) = \left\{ \begin{array}{ll} 1, & x > x_{th} \\ 0, & \text{otherwise} \end{array} \right\}$$

$$WAMP = \sum_{k=1}^{N-1} f(|x_n - x_{n+1}|)$$

This parameter is related to the muscle contraction levels.

Frequency Domain Features

The analysis of the Power Spectrum Density (PSD) of the sEMG signal is often performed to estimate the extent of the fatigue phenomenon. As a matter of fact, during fatiguing contractions the PSD content shifts toward lower frequencies. Therefore, the following parameters could be good estimators of the skeletal muscle fatigue [19].

Median Frequency. Median Frequency (FMD) is the frequency at which the power spectrum (P_j) is divided into two areas of equal power:

$$\sum_{j=1}^{FMD} P_j = \sum_{j=FMD}^M P_j = \frac{1}{2} \sum_{j=1}^M P_j$$

Mean Frequency. Mean Frequency (FMN) is the average frequency, such as the ratio of the sum of the signal power spectrum multiplied for the respective frequency to the overall sum of the power spectrum:

$$FMN = \frac{\sum_{j=1}^M f_j P_j}{\sum_{j=1}^M P_j}$$

1.3 Average Threshold Crossing (ATC)

In the field of movement pattern recognition, in order to infer the contraction force of the skeletal muscles the Surface ElectroMyoGraphic signal (sEMG) has to be acquired, subsequently processed and transmitted to an external workstation capable of getting the information required. The contraction force could be estimated for example using time domain features such as the Root Mean Square (RMS), as it was previously explained. Nevertheless, this process is extremely expensive in terms of power consumption.

The *Average Threshold Crossing technique* (ATC) could be an excellent solution since it allows the reduction of the amount of data to be managed and consequently the reduction of both circuit complexity and low power consumption. It consists of the generation of an event every time the sEMG signal exceeds a fixed threshold. As shown in figure 1.11, thresholding the total sEMG signal, the Threshold Crossing (TC) signal is obtained, which is defined as a quasi-digital signal since the pulse sequence includes only information regarding time but not the signal amplitude. The signal is proved to be highly correlated to the firing rate of muscle motor units and accordingly to the muscle contraction force [20].

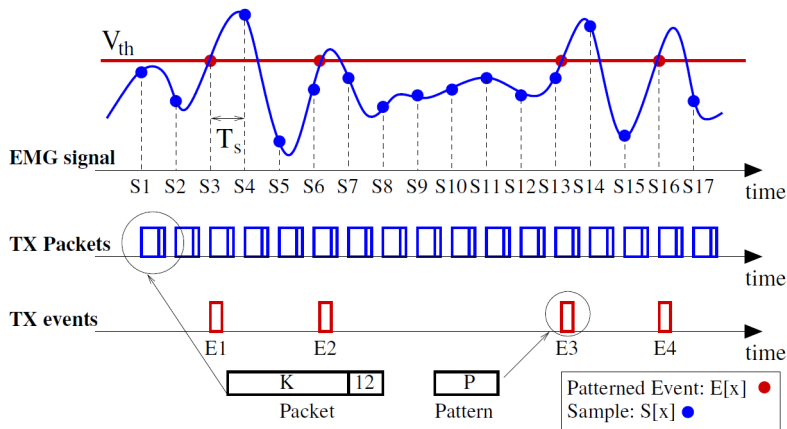


Figure 1.11: Average Threshold Crossing (ATC) technique [20].

As a matter of fact, the sEMG acquisition unit architecture is extremely simplified, since it does not require the Analog to Digital Converter (ADC), the clock generator and generally speaking complex logic to handle the data. Its three main components are instead the differential amplifier, the comparator, which compares the signal of interest to a defined voltage threshold (V_{th}) and a transmitter unit to send the data to the workstation. Previous studies [20], [21] demonstrated that

the number of ATC events increases as the force rises during isometric and isotonic contractions, allowing a 0% error rate force levels discrimination with a difference weight of 6 kg.

ATC approach, as it has been compared to the ARV parameter, is proved to be robust to wideband noise, almost not affected by the distortion of the signal and independent from a small random loss of events in the estimation of the muscle contraction force [21].

Nevertheless, the ATC technique presents some drawbacks since it does not include all the time and frequency information which could be extracted from the original sEMG signal. Therefore, it cannot be used for example in the diagnosis field, where the standard analysis of the morphology of the sEMG signal is required. Moreover, the choice of the threshold is extremely critical, since the number of spikes generated clearly depends on it. Therefore it should be set very carefully, taking in consideration the intrinsic variability of the sEMG signal.

1.4 Functional Electrical Stimulation (FES)

Functional Electrical Stimulation (FES) is a technique commonly employed in the recovery of patients affected by spinal chord injury and stroke, which cause the impairment of upper motor neurons and/or lower motor neurons and consequently the paralysis of upper and/or lower limbs [22]. Functional electrical stimulation consists of a series of low energy pulses applied to the affected limb of the patient through surface electrodes or more rarely intramuscular electrodes, causing muscular contraction and accordingly functional limb movements.

1.4.1 FES Parameters

The main FES parameters are: pulse amplitude, width, pulses waveform and frequency. The pulses waveform can be monophasic, biphasic or polyphasic (Fig. 1.12).

Most of the FES devices present in the market employ *biphasic rectangular pulses*: right after the positive phase, a negative pulse is provided, allowing an active discharge to avoid electrolytic effects or skin irritations [25].

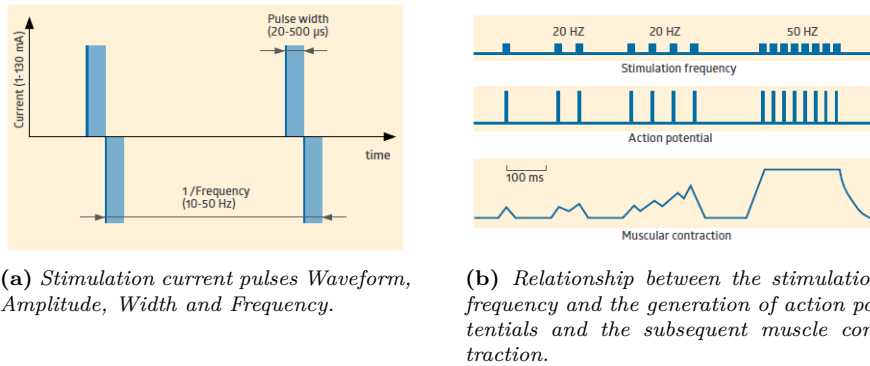


Figure 1.12: FES parameters description [25].

Stimulation frequency, meaning the number of pulses per seconds, depends on muscle fibers distribution and it is highly correlated to the muscle strength achieved; it should be high enough to guarantee a tetanic contraction. Therefore it normally ranges from 10 Hz to 50 Hz. *Current amplitude* typical values are generally set between few and tens of mA, depending on the subject and the muscle type. Alternating current is used. *Pulse width* fluctuates between tens and hundreds of μs . Nevertheless, electrical stimulation parameters must always be adjusted individually according to one's muscular constitution, physical nature, stimulus threshold and individual pathology.

FES therapy is generally used in conjunction to a comprehensive rehabilitation program, especially as a treatment for foot drop, where there is a dysfunction during the foot lift while walking [23].

FES devices are nowadays small and quite easy to use permitting in most of the cases, after an initial parameters set-up by specialist medical staff, the performance of the treatment at home. According to several studies and researches, FES is proved to be effective, allowing improvements in the performance of Activities of Daily Living (ADL), muscles strengthening, Range Of Motion (ROM) increase. Since FES stimulates motor neurons, it is fundamental the integrity of the nerve fibres between the spinal cord and the muscle and of the muscle itself [24].

1.5 Range Of Motion (ROM)

Range Of Motion (ROM) is the measurement of movement around a joint or body part (an example is provided in figure 1.13). Paralyzed patients have reduced flexibility in certain joints, resulting in a limited or even zero Range of Motion. In order to mobilize the affected joint, the therapist may help the patient performing

specific exercises: Passive Range Of Motion (PROM) exercises consist of the passive stretching of the patient limb by the therapist while Active Range Of Motion (AROM) exercises are performed by the patient independently, with no medical assistance [26]. The dynamic tracking of angle joints is widely used in rehabilitation processes in order to verify the effectiveness of physiotherapy or as an additional parameter in the diagnosis of motor diseases.

Nonetheless, in this thesis project, two electrogoniometers are used to assess the similarity between the degree of movement of controller and controllee limbs. With this approach the ATC-FES system could be validated.

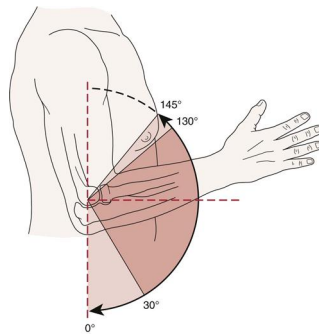


Figure 1.13: Example of elbow joint ROM [26].

1.5.1 Articular Goniometers

Digital goniometers are thus fundamental to track the dynamic movement of the patient joint. The working principle is based on the conversion of a definite voltage level to the desired joint angle. Sampling the voltage continuously allows the dynamic angle tracking.

Most of them are resistive transducers, such as potentiometers and strain gauges: the joint angle movement causes variations of the internal resistance of the device positioned in the joint's rotation point, which is detected through a voltage output and subsequently converted into the angle value.

1.5.2 Rotary Encoder

An encoder is a mechanical motion sensor: mechanical motion information (position, speed, distance, and direction) is converted into electrical signals [27]. Rotary encoder, in particular, performs the conversion of the motion data of a shaft or axle. It has a disc with a circular holes pattern, that rotates freely around a shaft. The transduction of its position is achieved by a source that emits a signal on one

side of the disc, which is then received by a detector on the other side when the signal is allowed to pass by the holes. Rotary encoders can be defined as incremental or absolute.

Incremental Encoder

An incremental encoder generates a pulse for each incremental step in the holes pattern, providing the relative position of the disc. Nevertheless, to determine the disc direction of rotation, two detectors and two signal sources (Channel A and B) are necessary. The decoding of the resulting two quadrature outputs, permits the monitoring of both direction (clockwise or counterclockwise) and relative position, with the production of a count up or count down pulse as appropriate (Fig. 1.15).

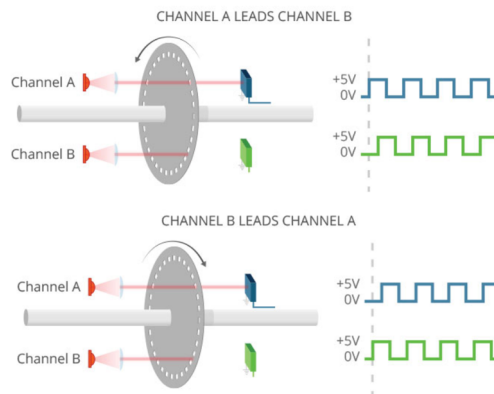


Figure 1.14: Encoder functioning. If A leads B, signal A shows a rising edge before signal B and the disk is rotating in a counterclockwise direction, otherwise the direction is clockwise. [27].

Capacitive Absolute Encoder

Absolute encoders generate a unique digital code for every possible position of the shaft. They have a greater resolution, compared to incremental encoders, which is expressed in bits, allowing extreme precision measures. According to their working principle, they can be optical, magnetic, fiber optic and capacitive [28]. Capacitive encoders have a transmitter which allows the propagation of an high frequency signal to the rotor. The signal modulations obtained through the etched sinusoidal pattern on the rotor surface, reach the receiver and are then elaborated into the specific absolute position by on-board electronics.

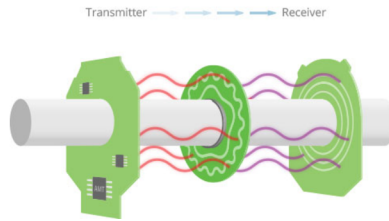


Figure 1.15: Capacitive Encoder. [27].

Chapter 2

State of Art

2.1 sEMG Acquisition Systems

The acquisition of the electromyographic (EMG) signal has become fundamental both in rehabilitation engineering and medical research. One of its main applications is the myoelectric control of prostheses thanks to the physiological information included in the EMG signal. This concept was first introduced in the late 1940s and was greatly developed during 1960s, 1970s and 1980s [41]. Nevertheless, the EMG signal has to be processed in order to remove the unwanted noise and use only the signal of interest. The main noise sources are electromagnetic devices (*ambient noise*) whose dominant frequency is 50 Hz and the difference between the electrode and the skin surface impedances. Firstly premising to normally use bipolar electrodes in prosthetic devices, the signal conditioning consists of the following stages summerised in figure 3.17:

1. *Instrumentation Amplifier*: it realises the differential amplification by subtracting the two input signals. In this way the ambient noise, which is common to both inputs, can be removed. The effectiveness is measured by common mode rejection ratio (CMRR), which should be at least 90 dB.
2. *Low Pass Filter*: it eliminates the frequency components higher than the cut-off frequency (f_c), corresponding to the noise produced by nerve conduction and high frequency interference. f_c is set around 500 Hz.
3. *High Pass Filter*: the frequency components with a value lower than the cut-off frequency are attenuated, such as DC offsets, sensor drift on skin (motion artifacts) and temperature fluctuations. f_c is set around 10 Hz.

4. *Amplifier*: using for example a non-inverting amplifier the EMG signal can be amplified with a gain that depends on the muscle selected. Since its original amplitude is about 1-10 mV, the amplifier gain ranges from 500 to 10000 [38].

The use of a notch filter to remove the power line interference (50 Hz), is generally avoided since the EMG signal provides a relevant contribution around this frequency.

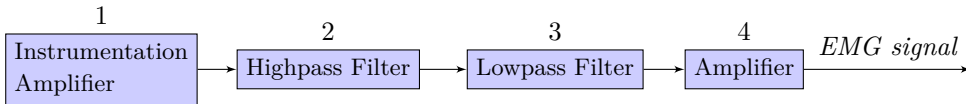


Figure 2.1: EMG Conditioning Stages.

After the fourth stage the analog EMG signal is ready to be analysed for the designed applications. The obtained analog signal has to be subsequently digitalised by an ADC (Analog to Digital Converter). According to the Nyquist Theorem, the signal is thus sampled with a sampling rate at least twice the highest analog frequency component (*Nyquist Frequency*) in order to avoid the signal distortion (aliasing). The Nyquist frequency is about 500 Hz for the sEMG signal, therefore the sampling frequency is typically set at 1000 Hz. The amplitude voltage resolution depends on the ADC number of bits and voltage range. Commonly the ADC works with a resolution of 8, 12 or 16 bits for a range between -5 and +5 Volts [42]. The resulting digital signal is then transmitted to an external workstation that allows powerful computation to extract and elaborate important signal information. The transmission is usually wireless so that the overall system can be wearable. Hence power consumption becomes one of the main issues, especially in real time applications.

2.2 ATC technique applied to sEMG

Through the ATC technique it is possible to obtain similar properties to the most common EMG features which are traditionally used to classify different muscle contractions such as MAV, RMS, envelope and WAMP [42]. As a matter of fact, correlation coefficients between ATC and the other EMG features are proved to be high (between 90% and 95%). Therefore, the ATC technique can be employed in pattern recognition with the advantages of low power consumption and high robustness to interferences. This goal is achievable because this technique generates from the sEMG signal an event sequence that requires only time dimension but not amplitude. ADC, clock generator and complex logic are not necessary and hence avoided, resulting in circuit complexity, size and power consumption reduction.

ATC parameters should be set in order to optimize the signal acquisition for the specific application. The *time window* should have a length wide enough to ensure a reliable discrimination of muscle contraction levels but also short enough to allow an acceptable real-time performance. Typical values used for the muscle contraction force detection ranges from 50ms to 200ms. The voltage *threshold* should be a compromise between an high value that guarantees the noise avoidance and a low value that increases the system responsiveness to muscle contraction. This value should be indicatively set 100 mV greater then the EMG baseline.

2.3 FES-sEMG systems

Functional Electrical Stimulation (FES) is usually employed in artificial motor control of the paretic or plegic upper limbs. In order to restore motor functions in people affected by spinal chord injury (SCI) and stroke, FES parameters should be individually set to guarantee a comfortable and effective muscle contraction. For example, in SCI people the current intensity necessary to produce the desired movement is greater then in healthy individuals, due to their inferior muscle mass.

FES-sEMG Feedback Systems

Frequently, *closed-loop feedback systems* are used; the system's parameters vary according to the joint angle or electromyographic signal as a result of the residual muscle activity in the affected limbs. The main activities performed in FES rehabilitation programs are handgrip, hold and release objects, lateral gripping.

In some neuroprostheses the stimulation is controlled detecting movements by a sensor: when the joint angle reaches a certain value or a specific contraction pattern is observed, the stimulation is triggered (Fig. 2.2). This feedforward control allows the performance of more precise movements in a shorter time execution and avoids the stimulation of the wrong muscles.

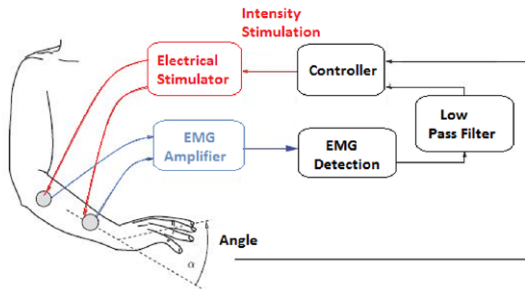


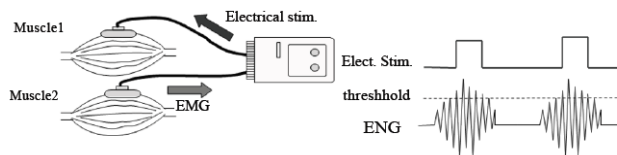
Figure 2.2: sEMG controlled FES system [44]. The electromyographic signal acquired triggers the functional stimulation after being processed and contributes to the FES parameters adjustment together with the joint angle signal.

Contralaterally Controlled Functional Electrical Stimulation (CCFES)

This stimulation therapy is proposed to patients affected by hemiplegia in the upper limbs. The contralateral unimpaired hand movement controls the intensity stimulation of the affected limb. Thus patients are able to perform their daily exercises autonomously moving their healthy limb which is covered by an instrumented glove. The glove shown in figure 2.3, has three band sensors that detect the muscular activity of the non-paretic hand.



(a) CCFES system set-up.



(b) CCFES functioning system.

Figure 2.3: CCFES description [45]. As it can be seen in 2.3b, the EMG signal from the non-paretic hand (Muscle1) is acquired, thresholded and used to set the proper FES parameters for the affected limb (Muscle2).

Rehabilitation systems based on communication between two people

Other rehabilitation devices use the simultaneous cooperation between the therapist and the patient. For example in the system proposed in figure 2.4, the multi-channel sEMG acquisition from the therapist is given to a learning machine

which states the relationships between muscle contraction patterns and joint motion. Through a stimulation model, the therapist motion is converted into electrical stimuli given to the patient. This rehabilitation procedure ensures the effective therapist-patient communication of motor information.

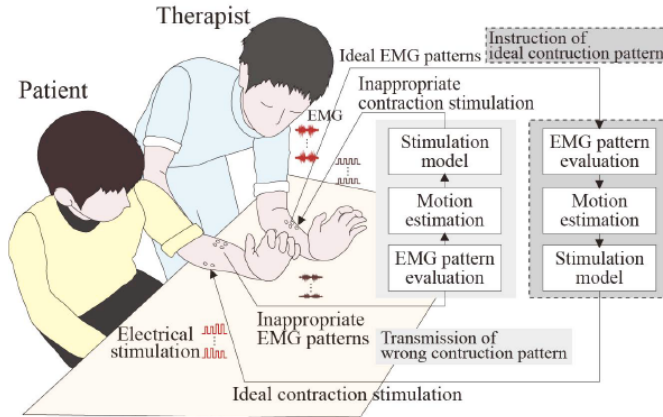


Figure 2.4: Direct rehabilitation method based on the use of FES and EMG [46]. The EMG signal is acquired from the therapist, capable of an ideal contraction pattern, and subsequently evaluated to elaborate the right stimulation pattern for the patient. Eventually, information on inappropriate EMG patterns are transmitted from the patient to the therapist.

2.4 Features of absolute encoders and their role in human joint angles analysis

According to the technique used to translate mechanical position information into an electric signal, absolute encoders can be classified into optical, magnetic, fiber optic and capacitive. The most common device available on the market is the *optical encoder*, which uses infrared light and phototransistors as source signal and output detection. It is used especially in applications that require an extreme accuracy.

Magnetic encoders are usually employed in extreme environments; severe temperature and humidity conditions, presence of airborne contaminants. *Fiber optic encoders* are used in presence of flammable gasses since they are called "explosion proof". A relatively new type is the *capacitive encoder*, which is a good compromise between high accuracy and resistance to adverse conditions, even though it cannot be employed in explosion-proof applications [27]. They are employed in applications which require high precision and durability. [28].

As a matter of fact, capacitive encoders unlike optical ones do not require an optical disk, which is a great advantage in terms of resistance, robustness to environmental contamination, temperature stability and power consumption and they still provide high resolution. Moreover, they are quite robust like magnetic encoders, but unlike the latter capacitive encoders provide higher resolution and lower sensitivity to magnetic interference. Therefore, capacitive encoders are capable of providing high precision without sacrificing robustness even though they are quite susceptible to noise and electrical interference.

Absolute encoders can be used as electro-goniometers, by converting the actual absolute level into the correspondent angular position. In particular, they can be employed in articular goniometers since they are capable of providing the high resolution necessary for the body joints measure and tracking. Generally speaking, the analysis of human joint angles could be employed to diagnose pathological knee joint conditions and motion disorders by measuring the Range Of Motion (ROM). It has important orthosis applications as well.

Chapter 3

System Architecture

The overall system is graphically described in figure 3.1. It is composed of an acquisition board which acquires the sEMG signal from the controller by means of two active electrodes placed on the specific muscle belly (biceps brachii muscle in this case) and a reference electrode placed on a non conductive skin portion. The Micro Controller Unit (MCU) on the board counts the number of TC events occurring within the chosen time window (130 ms) and sends the information to the Bluetooth device RN4020[®], which in turn sends the data to the CC2540[®] dongle. Simultaneously the angle signals of both controller and controlee are acquired through an Arduino[®] micro board which is directly connected to the computer via USB cable. In Matlab[®] and Simulink[®] environment the TC data acquired are converted into the correspondent current pulse which. The stimulator will eventually deliver the stimulation using stimulating surface electrodes. The acquisition of the TC information and the angle data is controlled by a Graphical User Interface (GUI).

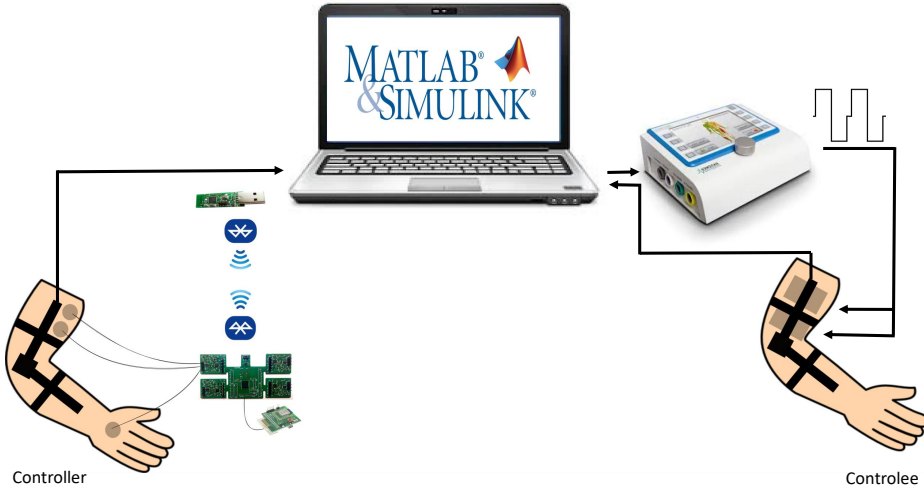


Figure 3.1: General scheme of the system functioning

3.1 System Architecture Description

The overall systems performs five main phases such as *Aquisition*, *On board elaboration*, *Transmission*, *Processing* and *Actuation* which are illustrated in figure 3.2.

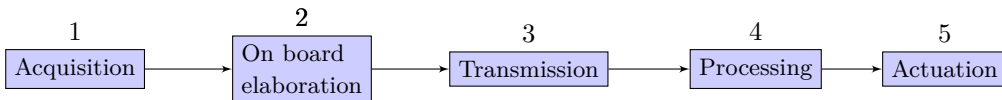


Figure 3.2: General work-flow of the system functioning

First the surface electromyographic signal is acquired from the therapist and elaborated in the acquisition board so that counts the number of TC events produced within a certain time window and subsequently transmits it to the elaboration unit through Bluetooth Low Energy (BLE). Afterwards, the FES therapy is elaborated, such as a series of low energy current pulses whose number, timings and amplitude are based on the count of TC events that has occurred. The current stimuli are then sent to the patient limb using stimulating electrodes connected to the RehaStim2[®] stimulator.

3.1.1 Acquisition Board and Data Transmission

The acquisition Printed Circuit Board (PCB) used in this project shown in figure 3.3, has an *analog part*, to which four differential acquisition channels belong and a central *digital part*, which counts and sends the data.

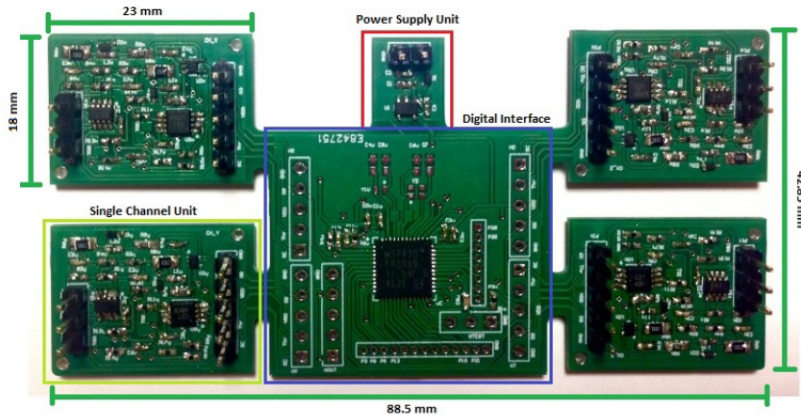


Figure 3.3: The PCB used to acquire the sEMG signals [39]. It includes a power supply unit, a central digital interface and four possible analog front-end channel units

Analog section

The signal conditioning is already performed on the board, so that it is possible the subsequent calculation of the number of TC events and the sending via BLE of only the ATC information. In this way the *power consumption* is considerably reduced. First, there is a *band pass filter* with cutoff frequencies of 34 Hz and 397 Hz. The lower one removes the motion artifacts while the highest one deletes the frequencies not interesting for the sEMG signal, since the superior limit of its bandwidth is about 400 Hz. Afterwards, the signal is amplified by an *instrumentation amplifier* (INA321), which has a gain of 922, obtaining the desired sEMG signal. At this point it can be finally compared to a determined threshold by a *voltage comparator*, so that the TC signal is generated.

In order to obtain the desired quasi-digital signal, any time the sEMG signal overcomes the value of the threshold plus (or minus) the upper (or lower) hysteresis value of the comparator, its output changes state. The hysteresis comparator value is set to 15 mV for both positive and negative since it has been evaluated as a good compromise between TC events detection sensitivity (lower hysteresis values) and low susceptibility to noise (higher hysteresis values) [43].

The two signals, sEMG and TC, are both the output of the four analogic acquisition

channels. The board is powered with a voltage of 3.6 V, value that can be supplied by a portable battery in a wearable system.

Digital section

The digital part includes the MSP430FR5969 (MSP430TM family) *Micro Controller Unit (MCU)* produced by Texas InstrumentsTM. Its main tasks are: providing the comparator the voltage threshold, counting the number of TC events, handling the data transmission through the communication with the BLE module connected to the board and eventually, if requested, using the internal Analog to Digital Converter (ADC) to digitalise the sEMG signal. This last feature is not necessary for the system functioning but can be useful to assess the correct behaviour of the board.

As previously explained, the reference voltage is supplied to the voltage comparator by the MCU. Thus, a *Digital to Analog Converter (DAC)* for every channel is needed to convert the digital voltage signal provided by the MCU, to the corresponding analog signal. In order to achieve this purpose, the integrate MAX5742 produced by MAXIMTM, containing four DACs, is employed. It communicates with the MCU via SPI protocol, through which it receives the commands and the digital voltage threshold. Eventually it sets as output the analog signal. The default threshold value is set at 1.9 V.

3.1.2 Data Elaboration and Stimulation

ATC data generation

As introduced in section 3.1.1, the count of the number of TC events is executed on board by the MCU. Every time the sEMG signal crosses the voltage threshold, an impulse is generated. The MCU counts the number of impulses occurring in a time window of 130 ms, for each channel individually. It was chosen a time lapse of 130 ms, since it is proved to be the right compromise between a fast data elaboration and a sufficient number of events detected to discriminate several force levels [40].

Data Transmission

The obtained data are then transmitted to the workstation by *Bluetooth Low Energy (BLE)* protocol. The MCU communicates with the RN4020 module (produced by Microchips[®]), which is connected to the acquisition board. The bluetooth dongle CC2540, produced by Texas InstrumentsTM is instead paired with the Matlab[®] workstation. The roles in the communication between the two bluetooth modules, define the peripheral RN4020 as the server and the central CC2540 as the client. The commands are controlled by the user through a Graphical User Interface implemented in Matlab[®], version 2017-b. Thanks to the GUI, the user choose the

operation that he wants to perform and the relative commands are sent by the CC2540 dongle to the RN4020 module. The latter informs the MCU about the action needed and, after the acquisition, stores the data in the server, which is then transmitted to the client and eventually elaborated by the workstation. The possible actions that the user can control by sending the relative command through the bluetooth communication protocol are:

- Start of the TC events acquisition
- Stop of the TC events acquisition
- Setting of a specific threshold value

ATC Data Elaboration and FES Therapy Elaboration

As previously introduced, the data elaboration is controlled by a GUI implemented in Matlab and performed in Matlab[®] and Simulink[®] environment. Through Simulink[®] simulations it is possible to receive, send and eventually elaborate the data. It was chosen this solution since the RehaStim2[®] stimulator has a predefined Simulink block that receives the stimulation parameters in input and send them to the corresponding external device using a serial port (Fig. 3.4), with the possibility of controlling the stimulation pulse by pulse

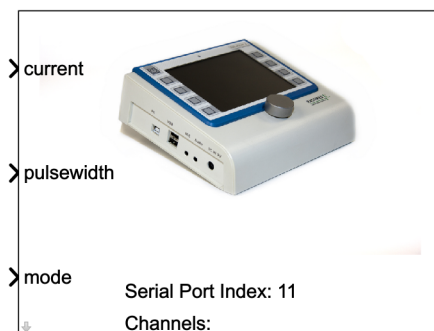


Figure 3.4: RehaStim2[®] Simulink[®] interface.

The Simulink simulation created open two COM ports with the serial configuration shown in Table 3.1: one permits the serial communication with the CC4020 and indirectly the acquisition board while the other manages the stimulation as just explained.

Table 3.1: Rehasstim Stimulator[®] and Dongle CC2540 serial COM port configurations.

| <i>Parameters</i> | <i>RehaStim</i> | <i>CC2540</i> |
|--------------------|-----------------|---------------|
| Communication port | COM6 | COM5 |
| Baud rate | 460800 | 115200 |
| Data bits | 8 | 8 |
| Parity | even | none |
| Stop bits | 1 | 1 |
| Byte order | - | LittleEndian |
| Flow control | none | none |
| Timeout | - | 10 (s) |

After the establishment of the bluetooth communication and the start of the simulation, the data arrive every 130 ms, containing the number of TC events occurred in this time window from each of the four channels. Initially, the workstation waits for four ATC packets, such as the number of events counted within 520 ms (four consecutive time windows). Afterwards, the median operator is applied to these values, in order to obtain a more reliable information about the muscle contraction and avoid possible outliers. After this initial buffering time, the data is elaborated every 130 ms, almost in *real time*, calculating a running median for the value which has just been read and the previous three ones.

At this point, according to the median of the TC events detected in 520 ms, the correspondent output current value is calculated. There are 9 possible current amplitudes to dispense: each one is referred to a certain TC events number interval. The correlation between ATC parameter acquired and stimuli to be delivered is defined in the initial calibration phase.

Calibration

The choices of the *TC events interval value* and correspondent *current amplitude value*, are made separately before starting the real stimulation. The TC events number intervals are calibrating first setting the right threshold for the specific therapist and then taking in consideration the TC events produced by the subject who acts as the therapist during a contraction. The current amplitude, is instead set evaluating the effects of different current amplitude stimulations on the person to be stimulated, such as the Active Range of Motion (AROM) reached and the comfort or discomfort reported by the subject. The median of the maximum TC events number generated during four contractions of a certain muscle will correspond to the maximum current amplitude decided for the stimulated person.

3.1.3 Actuation

RehaStim2™ Stimulation Device

The stimulation is actuated using a the certified medical stimulator RehaStim2 by the company HASOMED GmbH [35]. This portable device delivers low amplitude current pulses through its eight channels. The first four channels are controlled in current by a module while the last four ones are managed by another module.

Through an open communication protocol named ScienceMode2, the stimulator can be externally controlled via a USB serial interface, using its specific driver. The protocol can be managed by a Simulink interface block, that allows to set directly the stimulation parameters shown in Table 3.2 in real-time for every pulse individually.

Table 3.2: Technical specification of the RehaStim2 stimulator [35].

| <i>Parameters</i> | <i>Description</i> |
|------------------------|-----------------------------|
| Current | 0-130 mA |
| Pulse width | 0-500 μ s |
| Frequency | 1-50 Hz |
| Channels | 8 (2 current sources) |
| Serial Port | USB with galvanic isolation |
| Main pulse interval | - |
| Inter pulse interval | minimum 8 ms |
| Low frequency channels | optional |
| Low frequency factor | optional |

The current pulses have a biphasic shape; first a positive rectangular amplitude pulse with a certain pulse width is delivered and, after a fixed delay of 100 μ s, a second pulse of opposite amplitude (Fig. 3.5).

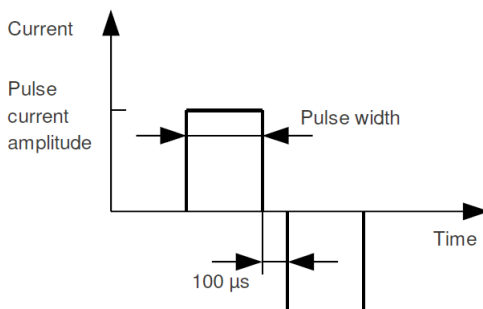


Figure 3.5: Characteristics of a current pulse delivered by RehaStim2 stimulator [35].

In order to guarantee the patient's safety, the skin resistance is checked before every stimulation pulse. If the resistance value is not acceptable, the stimulation will not occur.

The stimulator allows three pulse group modes, according to the number of repetitions of the pulse on the same channel:

- Single: the pulse is emitted only once
- Doublet: the pulse is repeated twice
- Triplet: the pulse is repeated three times

The pulse repetition occurs after an *inter pulse interval* (t_2). Since each pulse on each channel selected requires 1.5 ms even when the current delivered equals zero, the minimum inter pulse interval for each module is 8 ms (4×1.5 ms for each channel + 2 ms communication buffer). The channel list is instead processed considering a *main stimulation interval* (t_1). This value must be set according to the following equation: $t_1 \geq n \cdot t_2$, where n is the maximum of the selected pulse group modes used (1 for single mode, 2 for doublet mode and 3 for triplets). An example of a stimulation pattern is provided in figure 3.6.

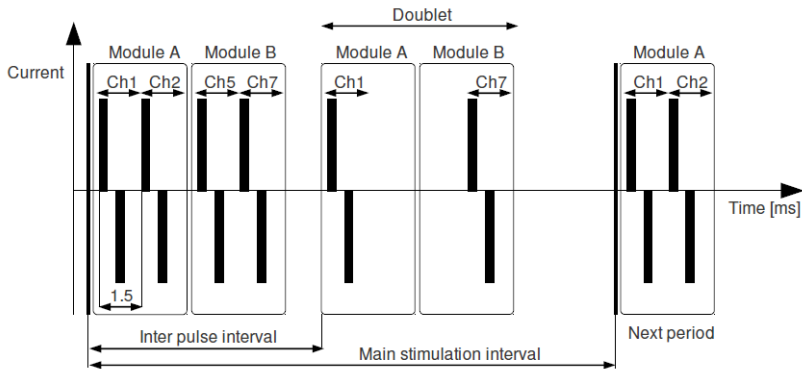


Figure 3.6: Example of a RehaStim2[®] stimuli pattern [35]. Channels 1, 2 from Module A and 5, 7 from Module B are selected and set with the same width and amplitude. The channels 1 and 2 mode is the doublet characterised by an inter pulse interval. The stimulation pattern is repeated after a main stimulation interval.

Eventually, the *low frequency channels* parameter indicates the channels having a lower frequency the others and the *low frequency factor* specifies how many times the stimulation is not delivered for those channels; the number ranges from 0 to 7. These are optional parameters, and their field is usually left empty.

3.2 Articular Electrogoniometer Realisation

In order to perform the angle trend tracking, an electrogoniometer was implemented. It consists of three main parts:

- *AMT20 absolute encoder*: the electromechanical transducer
- *Goniometer Case*: structure that guarantees the joint tracking
- *Arduino micro*: the angle elaboration unit

3.2.1 AMT20 Absolute Encoder

The AMT20 absolute encoder decodes the shaft position detecting the inner capacitance changes. The modulated signal produced when an high frequency signal reaches the rotor metal pattern, is then sensed by the encoder receiver and finally converted into output pulses by the CUI's proprietary ASIC (Application Specific Integrated Circuit) [27]. It has the following main features:

- **High resolution**: 12 bit, 4096 possible angular shaft, with an typical achievable angular accuracy of 0.2° .
- **Wide temperature range**: -40° - 125° , like magnetic encoder it is able to withstand adverse conditions such as extreme temperature and particulates.
- **Low current consumption**: inferior to 10 mA, unlike most optical encoders.
- **Programmable zero position**: it is possible to set automatically the initial position (zero position) of the encoder, from which starting detecting the different angular values.

The update of the 12 bit position in the Micro Controller Unit (MCU) register occurs every 48 μ s. Moreover, it is *lightweight* and its *small dimensions* allow to use it in a vast series of applications. It is easy to mount and noticeably *flexible* since its shaft sleeves and adapter permit to fit the encoder into several shaft sizes (Fig. 3.7).



Figure 3.7: AMT20 absolute encoder. [27].

Serial Peripheral Interface (SPI)

The AMT20 communicates its output to external devices thanks to the Serial Peripheral Interface (SPI) protocol, whose simplicity allows it to work at speeds even greater than 10MHz and to operate in full duplex mode (simultaneous communication in both directions). It has a *master-slave architecture* according to which the master is the acquisition device and the slave is the AMT20 encoder (Fig. 3.8).

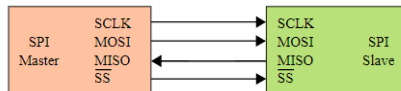


Figure 3.8: SPI Master-Slave architecture [32].

It is based on four signals:

1. MISO (Master In Slave Out): represents the master data output.
2. MOSI (Master Out Slave In): represents the slave data output.
3. SCK (Serial Clock): defines the timing of the transactions, it is set by the master.
4. CSB (Chip Select): defines the beginning and the end of the master-slave communication, it is set by the master and it is active low.

The encoder serial interface works with a data rate of 1 MHz. As it is shown in figure 3.9, 8 bits in a frame are transferred according to the big endian format, since the sequence of bits is ordered from the big end (most significant bit) while the least significant bit is in the last position. Data on the Master Output (MISO) is captured on the rising edge of the clock signal (SCK), while on the falling edge a new Master Input data is acquired. These operations are achievable if the chip select is low: as soon as it changes to the high state, the clock counter is reset.

Since the encoder has a resolution of 12 bits, the overall data consists of two byte, which thus have transmitted in two different frames: first the master will receive the Most Significant Byte (MSB), whose lower four bits are the upper four of the 12-bit position word and right after the Least Significant Byte (LSB), which refers to the lower eight bits of the 12-bit position word.

3.2.2 Angle Data Acquisition

The elaboration of the encoder absolute position is achieved using an Arduino micro device. It was chosen since it is the smallest Arduino implementation, permitting an easy integration into the electrogoniometer case. It communicates with the AMT20 through the SPI protocol: receives the data on MISO and send it to the matlab workstation via USB cable. The use of the SPI with a full duplex communication mode, implies the simultaneous exchange of information between master and slave: the master will submit a command and the slave will reply back with an acknowledge code before the data transfer.

SPISettings

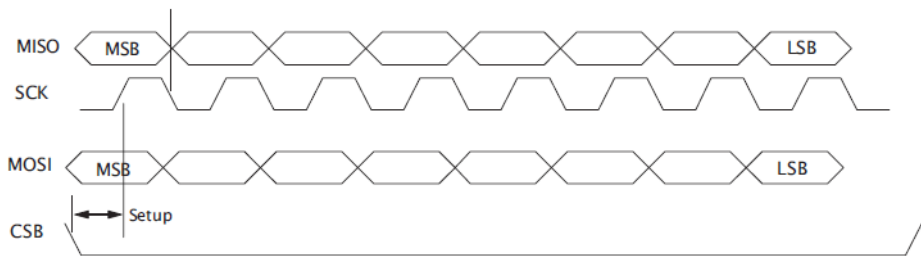


Figure 3.9: SPI timing diagram [33].

SPI commands

All the commands consist of 8 bits. The general principle is based on the submit of a **command** by the host, which is, in this case, the Arduino micro, and the following **response** of the encoder: If it is not ready it will send a *wait response* (0x05), otherwise it will submit the original command previously sent by the master.

- *No operation* (command 0x00): The master sends this command when no directions have to be transmitted, while receiving the data or while waiting for the encoder feedback.
- *Read position* (command 0x10): In order to receive the current position, the master sends the read position command and the encoder immediately reply

with the idle character. While reading the wait response (0x05), Arduino submits the no operation command. As soon as the slave echoes the read position request (0x10), the master sends 0x00 (no operation) and start receiving the MSB byte and subsequently the LSB byte while continuing issuing no operation. This process is repeat every 13 ms in order to have about 10 angle values within the ATC time window, which is 130 ms.

- *Zero point setting* (command 0x70): The master sends the command, and until it is not ready, the slave will continue submitting the *wait response* and Arduino the no operation command. When the encoder response is 0x80, the zero has been correctly set and the corrent position properly stored in the EEPROM.

3.2.3 Angle Data Elaboration

After reading successfully the MSB and LSB related to the 12-bit position word, the calculation of the corresponding angle is implemented in Matlab[®] and Simulink[®] environment. Ten 12 bit words are acquired through a serial port, all at once every 130 ms from the Arduino micro board with the configuration parameters shown in Table 3.3; first the MSB and LSB of every word are concatenated and the result is then converted into the corresponding integer number.

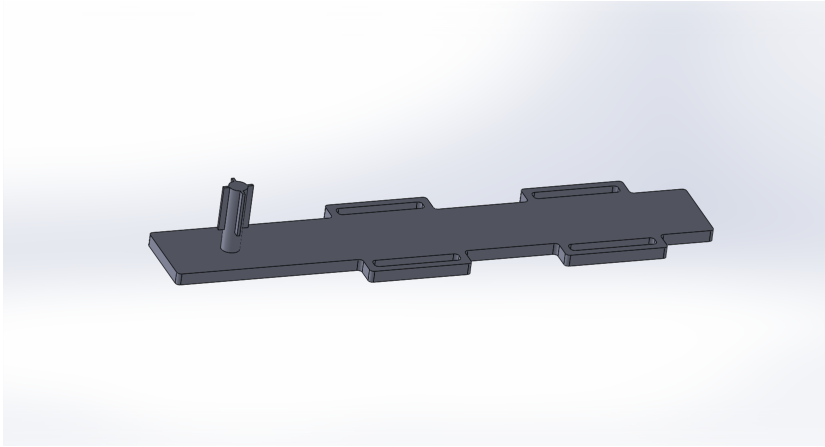
Table 3.3: Arduino serial COM port configuration.

| <i>Parameters</i> | <i>Value</i> |
|-------------------|--------------|
| Baud rate | 115200 |
| Data bits | 8 |
| Parity | none |
| Stop bits | 1 |
| Byte order | LittleEndian |
| Flow control | none |
| Timeout | 10 (s) |

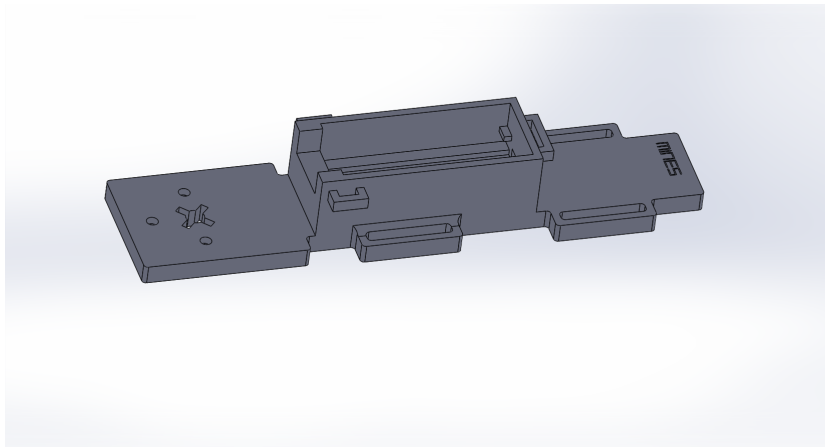
3.2.4 Articular Goniometer Case

In order to measure the joint angle, a proper goniometer case was realised creating first the CAD model with the software Solidworks[®]. It is composed of two beams, each one aligned and fixed by two elastic bands to one of the joint axis. The encoder rotation disc is fixed tightly to the shaft of one of the beams by means of small screws placed in its three circular holes, as it can be seen in figure 3.10. The beam in figure 3.10a is first inserted into the central slot and then the encoder is secured to it. The shaft presents four protrusions in order to perfectly adapt

its shape to the shaft sleeves. The Arduino micro is placed in the beam shown in figure 3.10b, so that it can be in close contact to the encoder. The case was designed so as to align the shaft to the rotation centre of the selected joint.



(a) *Beam with the shaft*



(b) *Beam to which the encoder is fixed*

Figure 3.10: Encoder CAD model created with Solidworks®.

Figure 3.11 shows the final aspect of the electrogoniometer and their positioning on the subjects limbs by means of four elastic bends.



Figure 3.11: Electrogoniometer final implementation.

3.3 Software control and elaboration of the operations

All the operations to be performed are handles in Matlab[®] and Simulink[®] environment. Through a GUI implemented in Matlab[®] it is possible to control the setting of the Bluetooth connection, the different stimulation parameters and the start and stop of the whole process. The process involves, as previously introduced, the simultaneous TC and angle data acquisition and the controlee stimulation and, once started, it is completely managed in Simulink[®] environment. Nevertheless, while the simulation is running, the actual data are stored in the Matlab[®] workspace and plotted in the GUI every 130 ms. Figure 3.12, shows the different roles played by Matlab[®] and Simulink[®] and the cohordination existing between them.

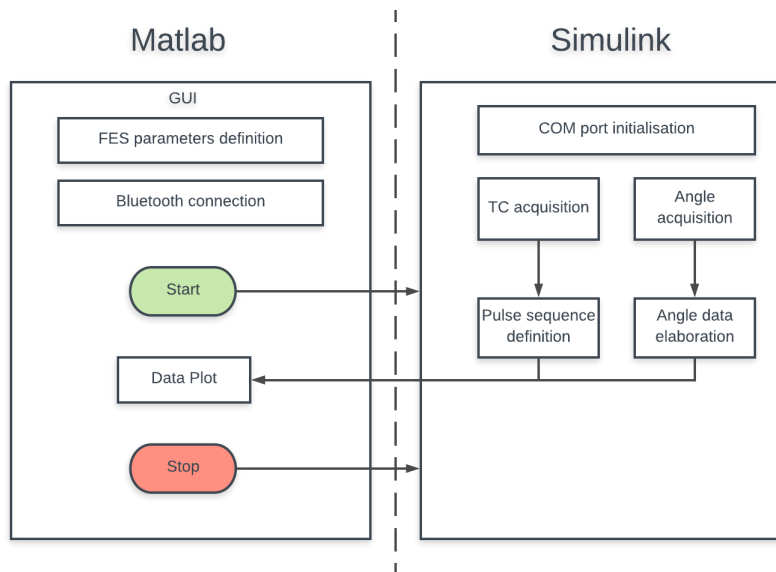


Figure 3.12: Actions and roles played by Matlab[®] and Simulink[®]

3.4 Matlab Graphical User Interface (GUI)

The user can easily choose the action to be performed through a Matlab[®] Graphical User Interface (GUI) that manages all the processes (Fig. 3.13). The main GUI sections are described below.

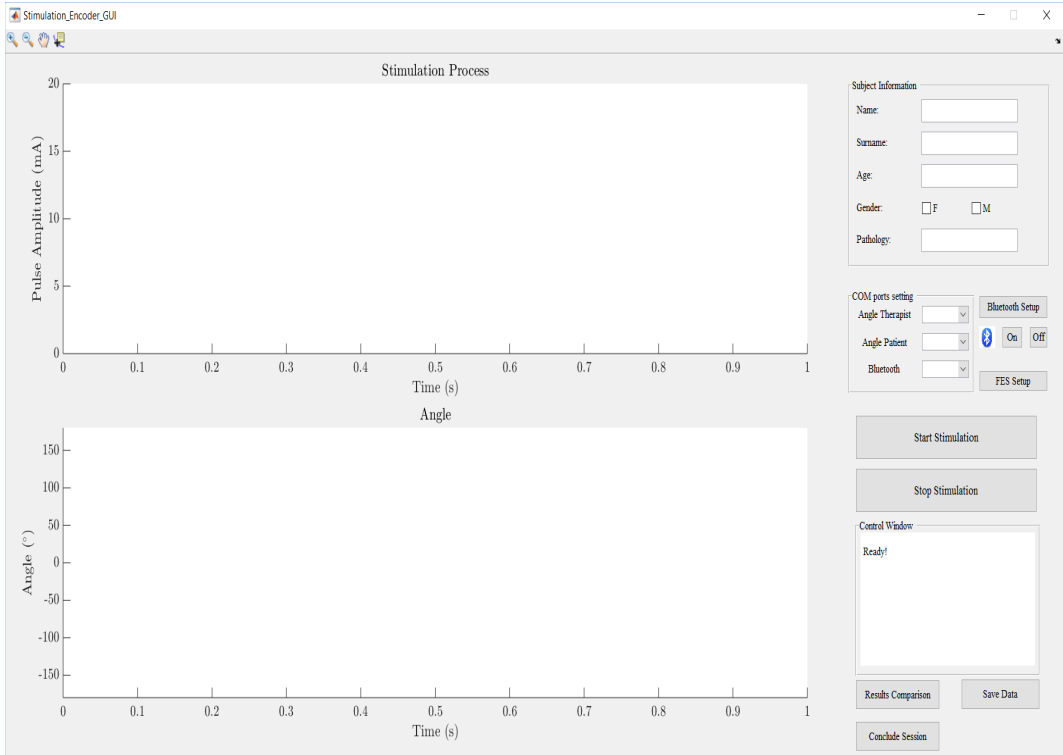


Figure 3.13: Main Graphical User Interface (GUI) created in Matlab[®] environment.

- *Subject information:* Information about the patient stimulated can be stored and subsequently save, since they are important in the statistical analysis.
- *COM ports setting:* This panel allows the choice of the correspondent serial ports automatically selected by the computer for the two angle trends acquisition and the Bluetooth connection.
- *Bluetooth Setup:* This push button allows the establishment of the connection between the two Bluetooth devices. The success of this operation is displayed in the control window.

- *FES Setup*: The callback function related to this button runs another GUI displayed in figure 3.14.

- *Start stimulation*: The callback of this button runs the Simulink Simulation: the COM ports of the goniometer and the stimulator are opened and, after an initialising phase, the data starts arriving. Every 130 ms the serial ports receive the angular and TC data. The angle tracking and the stimulation process are displayed in real-time in the two main graphics while the simulation is running.

- *Stop stimulation*: This button stops the stimulation, closes the Simulink models, disconnects the Bluetooth and stops the Arduino acquisition of the angular data from the encoder.

- *Result comparison*: After pushing this button, the result comparison GUI is displayed.

- *Save data*: After performing the stimulation and the simultaneous angle tracking, the relative data can be saved pushing this button and subsequently choosing the folder that includes the data.

- *Conclude session*: When the session is over, the user can push this button to interrupt the Bluetooth connection and finally close the GUI.

3.4.1 FES setup GUI

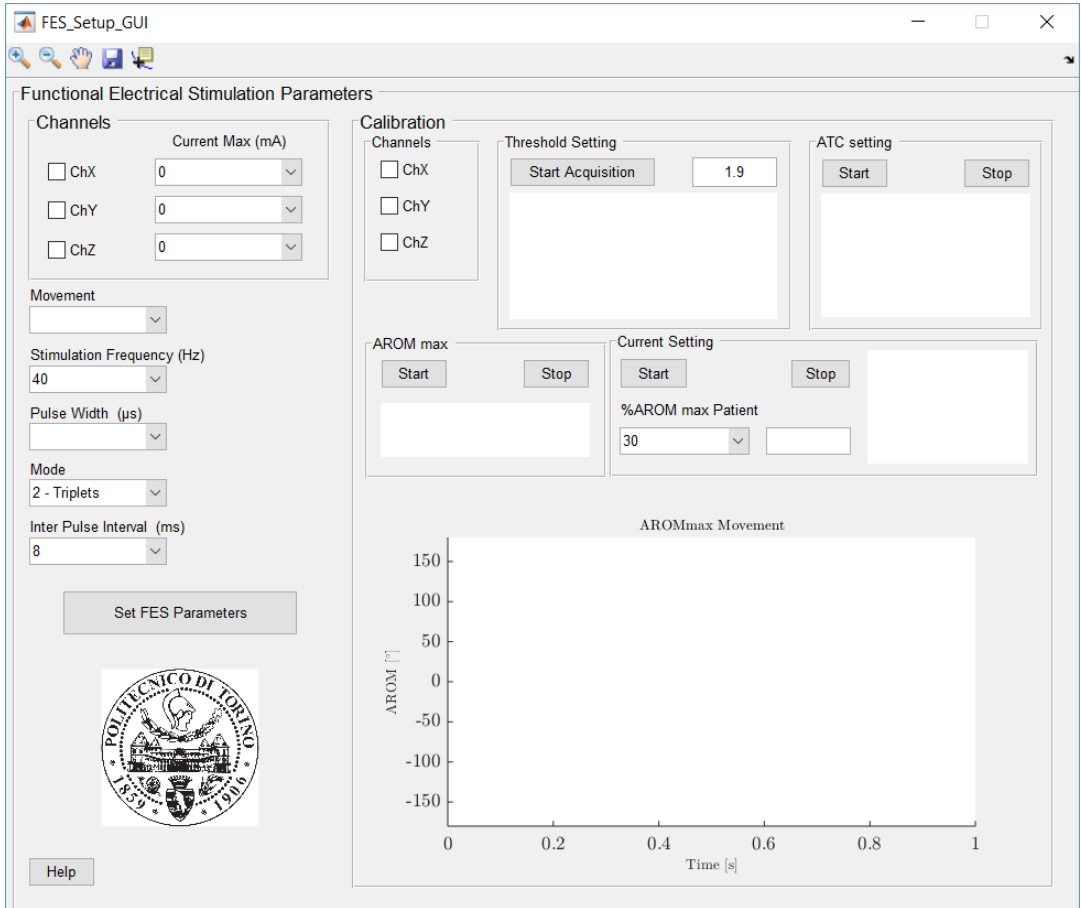


Figure 3.14: Graphical User Interface (GUI) used to set the proper stimulation and acquisition parameters.

This Graphical User Interface is recalled by the main GUI as previously explained and allows the performance of the initial calibration phase and the proper stimulation and ATC parameters setting. It is divided into two main sections:

1. *Setting of the stimulation parameters:* The FES parameters that cannot be changed once the stimulation has started, are chosen with the range values shown in Table 3.4.

Table 3.4: FES parameters initially set in the GUI by the user.

| <i>Parameters</i> | <i>Value</i> |
|---------------------------|--------------------------------|
| Channels selected | ChX, ChY, ChZ |
| Maximum current amplitude | 8-30 mA |
| Stimulation frequency | 10-50 Hz |
| Pulse width | 50-500 μ s |
| Mode | Single Pulse, Doublet, Triplet |
| Inter pulse interval | 8-80 ms |

Moreover, it is possible to choose a movement in the corresponding pop-up menu (elbow extension, elbow flexion, ankle dorsi-flexion, ankle plantar extension) to automatically set the proper FES parameters.

2. *Calibration:* Before the beginning of the stimulation, it is necessary a preliminary phase in which the proper stimulation features and the parameters related to the TC events acquisition are found, using the GUI functionalities in the following order:

Channels First of all, the TC acquisition channel must be chosen in order to perform the subsequent steps.

Threshold Setting As far as the acquisition part is concerned, it is necessary to set the right threshold for the selected therapist. Therefore, after applying the acquisition electrodes to the therapist skin surface and the start acquisition button, the system starts acquiring the TC events while the therapist is motionless in his resting position. If the number of events acquired within three seconds is zero, a lower threshold is set in the Micro Controller Unit (MCU). This procedure continues until an event is recorded.

At this point it is chosen a threshold value equal to the last one set plus the hysteresis value of the comparator (30 mV considering both negative and positive hysteresis). This is considered as the minimum threshold capable of guaranteeing no events in the resting phase and therefore the highest possible sensibility. The initial threshold can be easily established in the window nearby. If not set, the default initial value set in the MCU is 1.9 V.

ATC setting While the acquisition electrodes are placed and after pushing the relative start button, the therapist subject is asked to execute four movements that will be later performed during the rehabilitative exercises. When stopping the ATC setting, the median value of the maximum number of TC events occurred for each of the movement is calculated and used to set the TC number intervals corresponding to different current amplitude values used when executing the patient rehabilitation movement.

AROM max After pushing the relative start button, both the therapist and patient subject have to move their limbs in a way to reach their maximum AROM. When stopping the process, this value is calculated and used for the subsequent phase and for the final data analysis.

Current When starting, the patient is stimulated with a series of growing amplitude impulses. When the patient joint angle reaches a specific percentage of maximum AROM previously measured, the correct current amplitude is automatically chosen corresponding to the actual value increased by the 10% (upper limbs) or 20% (lower limbs). Otherwise if a satisfying value is reached but not equal or above the selected percentage of the maximum AROM and the patient feels discomfort, the stop button must be pushed and the current used will be the last one. It is possible to set the initial current value in the window nearby, otherwise the default initial value is 8 mA.

Above there is a graphic that displays in real-time the TC event number acquired or the AROM trends according to the selected setting, while in every calibration panel there is a window that displays the obtained data and the current status of the current process.

3.5 Matlab[®] and Simulink[®] code overview

Every element included in the GUI has a relative callback function in the GUI code that is recalled every time the action for that element is performed. The GUI callbacks referring to the start and the stop of the acquisition process are described in the following sections.

Start Stimulation Callback

When the Start Stimulation button is pushed, all the FES and TC parameters values previously stored in the Matlab[®] workspace are retrieved, the Bluetooth and goniometers COM ports are opened and flushed and the axis are initialised. Eventually some parameters are added to the Simulink[®] simulation:

- *Stop time*: it is set to "inf" so that the simulation will be executed until a stop command is sent.
- *Simulation Mode*: the normal mode is chosen since it offers the possibility to display results even if it is the slowest.
- *Init function*: an initial function which is run before the evaluation of the model block parameters, is assigned. This function is used to acquire the first four TC events, applying the median operator and give the resulting value to a model block. Eventually, the COM ports are deleted.

- *Start function*: a start function is called just before the beginning of the simulation. In this function a *listener* for a specific Simulink® block is created, which is a function that is executed every time a certain event occurs for a determined block. This procedure is used to plot the current angle and stimulation values in real-time.

At this point the "start" command is given to the Simulink® model.

Simulink® Stimulation model

The Simulink® model initially set the angle acquisition through the serial COM ports configuration block (Fig. 3.15). Afterwards, if the simulation time equals zero, the Subsystem block is executed (Fig. 3.16a). In this block the start command is given to the angle acquisition by sending the value 1 to the relative COM ports.

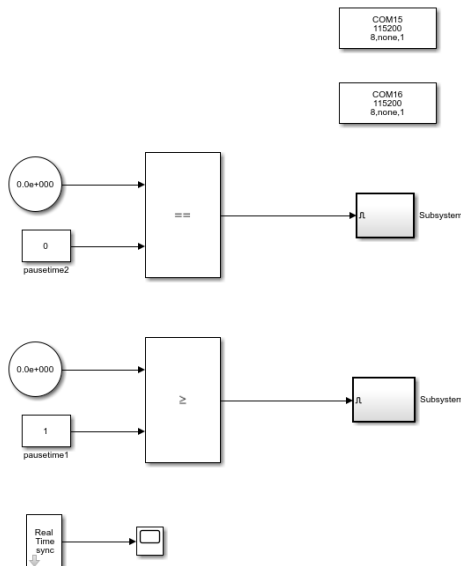
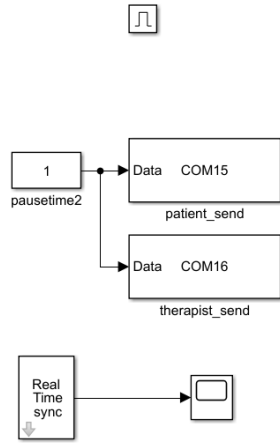
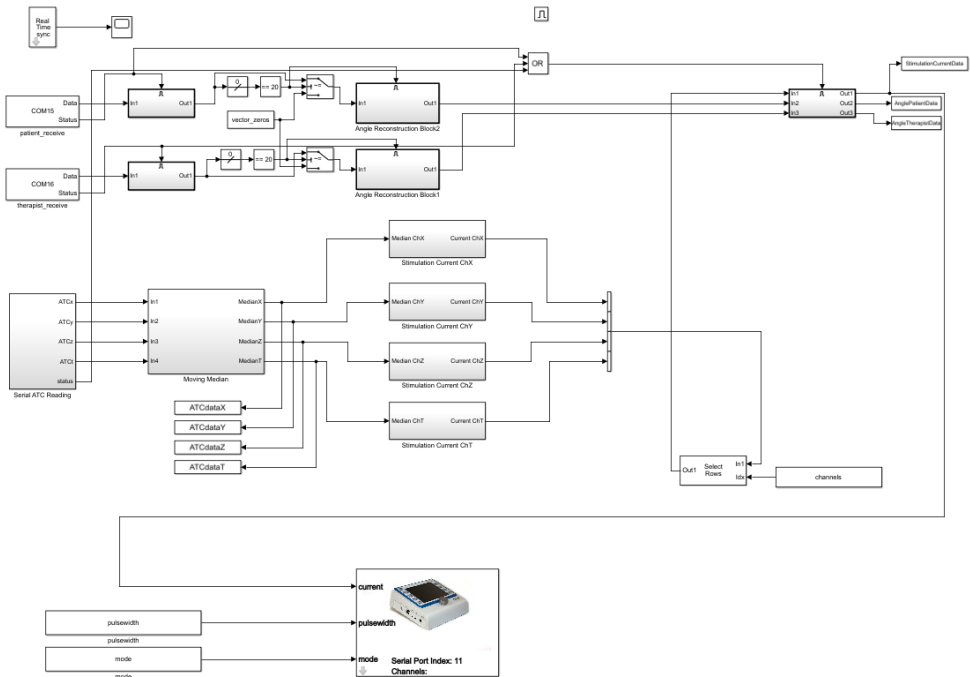


Figure 3.15: Simulink® stimulation top level model



(a) Subsystem block content



(b) Subsystem1 block content

Figure 3.16: Simulink® stimulation model blocks content

After one second, the Subsystem1 (Fig. 3.16b) is executed and the angles and TC events acquisition together with the stimulation start. At this point the following operations occur, illustrated in the general scheme in figure 3.17.

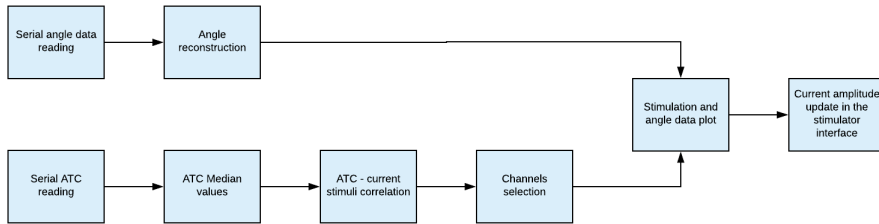


Figure 3.17: Flowchart of the actions performed once the stimulation is started.

- *Angle acquisition.* The two serial COM ports connected to the Arduino® board acquire 20 data every 130 ms. If the data reach the COM ports, the status of the serial receive block will be 1 and the succeeding steps will be triggered allowing the reconstruction of the 10 angle data through the conversion of the 2 bytes in input to the corresponding integer for each angle value (Angle Reconstruction Block1 and Angle Reconstruction Block2). If the number of data that reached the port is less than 20 a vector consisting of 20 zeros value is given as output. This control is useful at the beginning of the simulation, since it might happen the delayed arrival of the angle data.
- *TC data acquisition.* The Serial ATC Reading block receives and stores the number of TC events occurred within 130 ms, the Moving Median block applies the median operator to the four previous TC number values while the Stimulation Current blocks assign to the resulting TC number to a certain current amplitude value. Afterwards, according to the channels selected the relative current values are given to the Stimulator Interface block, together with the pulsewidth and the mode that are decided before the beginning of the simulation and kept fixed.
- *Real-time plot of the data.* Every time the Enabled Subsystem2 is executed, the function `updategraph` is recalled to plot the angle and stimulation trends relative to the last 13 seconds in the main GUI. This function is the listener created in the Start function for the cited block. The type of event for which the listener is evoked is specified as "PostOutPuts", such as after the the specified block's outputs method executes.

Stop Stimulation Callback

When the Stop Stimulation button is pushed, the Simulink® simulation is stopped and the relative model is closed. The TC events acquisition is stopped by sending the relative command to the bluetooth device and eventually the stop angle acquisition command whose value is zero, is sent to the arduino devices. The data referring to the acquisition (angles and stimulation trends) are automatically stored in the Matlab® workspace so that it is possible to save them pushing the relative save button after compiling the subject personal information.

3.6 Definition of the stimuli sequence from the TC data

As previously stated, the occurrence and the amplitude of the current pulses are controlled by the TC data acquired within the time window. Every 130 ms the correspondent pulse amplitude is computed and updated according to its relation between the TC events that has occurred. The parameters of this relation are preset during the calibration phase as shown by the scheme in figure 3.18.

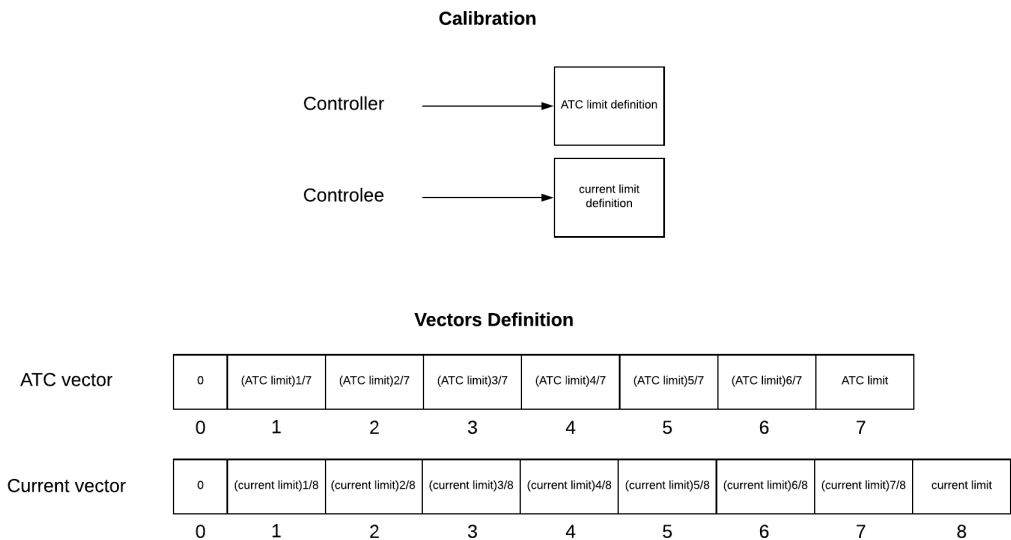


Figure 3.18: Setting of the acquisition-stimulation relation parameters during the calibration phase

As a matter of fact, during the calibration phase the median number of the maximum number of TC events is recorded from the controller subject, divided for the time window and defined as the *ATC limit*. Similarly the maximum current suitable for the controlee is determined and defined as the *current limit*. Right after their definition, these two parameters are used to set the corresponding ATC and Current vectors simply dividing their values for the chosen number of contraction force levels, which is nine. Eventually, during the real acquisition-stimulation process the correspondence between the ATC parameter acquired and the current to be delivered is determined as explained in figure 3.19: the ATC parameter acquired is compared to the ATC vector values and according to the resulting ATC level, the current amplitude is determined.

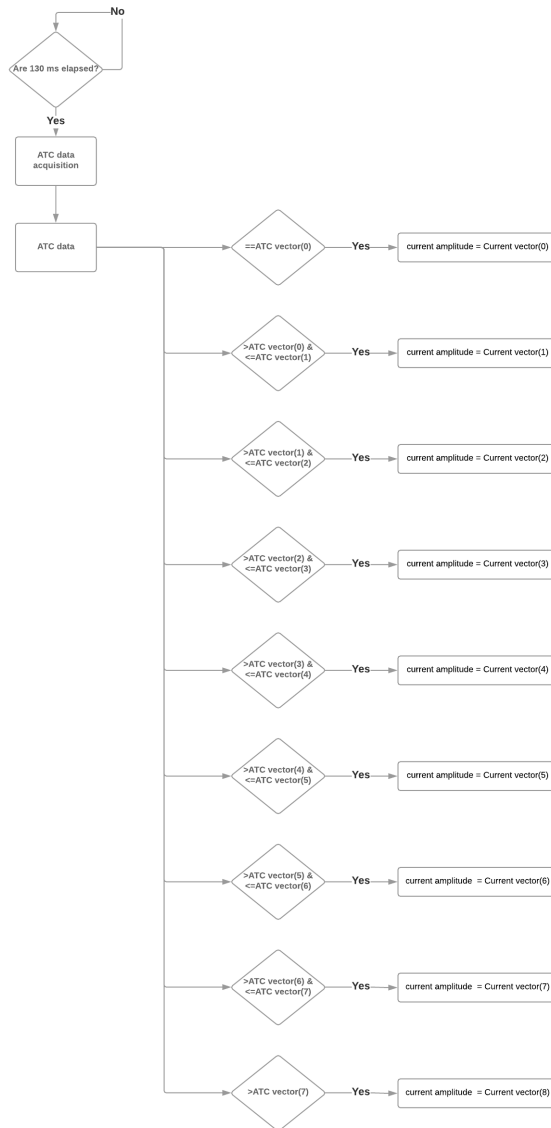


Figure 3.19: Flowchart of the ATC parameter-current amplitude definition during the acquisition-stimulation process.

Chapter 4

Experimental Acquisitions

Experimental tests have been performed acquiring simultaneously the two angles and the stimulation data, in order to assess the degree of similarity between controller and contreee movements. The performance was analysed in the case of *therapist-patient rehabilitation procedure* (one subject acting as the controller and the another as the patient under control), to avoid bias intrinsic in the self stimulation of the healthy subjects. To better ensure the effectiveness of the system, the subject under control was blindfolded, so that he could not be influenced by the timing and the entity of the controller's limb movement [29]. Both the sEMG signal acquisition and the delivery of the stimulation were performed in the dominant limb. Twelve tests were performed involving nineteen healthy subjects, 13 males and 6 females aged from 23 to 40 years old. The experiments were conducted ensuring the variety of the twelve couples and that the same person could play the role of the controller and the contreee at most once.

4.1 Acquisition Protocol Description

4.1.1 Acquisition Electrodes

The electrodes used to acquire the signal are produced by CovidienTM KendallTM, model H124SG (Figure 4.1). Their main features are collected in Table 4.1 [34]. They are disposable high quality electrodes, coated with solid hydrogel that guarantees their adhesion to the skin surface. The sensor is made of silver-silver chloride (Ag-AgCl). Their applications includes EEG, ECG and EMG and acquisitions.



Figure 4.1: CovidienTM KendallTM electrode

Table 4.1: KendallTM Electrodes Characteristics.

| <i>Parameters</i> | <i>Value</i> |
|---------------------|----------------------------------|
| Shape - Size | Round - 24 mm |
| Gel area | 201 mm ² |
| Sensor area | 80 mm ² |
| Backing material | Polyethylene foam (PE), white |
| Gel Characteristics | Conductive and adhesive hydrogel |
| Sensor | Polymer Ag-AgCl coated |
| Connector | Stainless steel |
| ACZ I impedance | 220 ohm |

Electrode Positioning

The acquisition electrode location and orientation are fundamental to acquire a proper sEMG signal. Since a bipolar configuration was used, there are two detecting electrodes that must be placed in the active area and a reference electrode positioned in a electrically neutral zone. The best detecting position is proved to be between the motor unit (innervation zone) and the muscle tendinous insertion along the longitudinal axis of the muscle and accordingly parallel to the direction of the muscle fibers [38]. The inter-electrode distance, meant as the distance existing between the centers of the two detecting electrodes, must range from 10 mm to 20 mm maximum.

The reference electrode is instead placed in an electrically neutral area far from the detecting electrodes. For the upper limb movements the reference electrode location used was the back of the hand while for ankle plantar flexion the medial malleolus and lastly for ankle dorsi-flexion on the kneecap.

Skin Preparation

A proper skin preparation is essential to for the quality of the sEMG signal obtained. Therefore the controller skin was cleaned with alcohol in order to reduce the impedance skin and subsequently allow the alcohol to vaporise so that the skin will be dry before the electrodes placement [38].

4.1.2 Stimulating Electrodes

HASOMED RehaTrode[®] electrodes are employed. They are reusable, self-adhesive and their active surface is covered with a conductive gel 4.2. The electrode size and form are chosen according to the selected muscles. A couple of electrodes are used for the stimulation.



Figure 4.2: Stimulating Electrodes produced by HASOMED RehaTrode[®]

Electrode Positioning

The two stimulating electrodes should be placed on the muscle belly, preferably with a handbreadth between them to optimise the stimulation effect. The position is adjusted individually according to the specific muscle taken in consideration. In order to assure the correct positioning of the stimulating electrodes, the muscle is stimulated with a train of increasing current amplitude pulses before the parameters calibration phase.

4.1.3 Movements Analysed

Four movements are analysed for the same subjects, among which two belonging to the upper limbs (elbow extension, elbow flexion) and two belonging to the lower limbs (ankle dorsi-flexion and ankle plantar extension). Each movement is performed consecutively on the same subjects 10 times during 3 different sessions. After every session there is a minimum time interval of 5 minutes, necessary to avoid the muscle fatigue. The angle data acquired were normalised to the maximum AROM of each subject previously measured. For each movement, the specific muscles that have to be stimulated, stimulation parameters and electrode size and

type are illustrated below, according to the suggestions of the Rehaslim operational manual [30]. The sessions are repeated alternating the four movements repetitions during the sessions in order to allow the proper stimulated muscle relaxation. The sessions and repetitions are performed according to the order explained in Table 4.2.

Table 4.2: Order of the sequence of session and repetitions in the chosen protocol. Each repetition consists of a sequence of ten consecutive movements. The repetition of each of the four selected movements has a different order through the three sessions.

| <i>Sessions</i> | <i>Repetition 1</i> | <i>Repetition 2</i> | <i>Repetition 3</i> | <i>Repetition 4</i> |
|-----------------|---------------------|-----------------------|-----------------------|-----------------------|
| Session 1 | Elbow flexion | Elbow extension | Ankle plantar flexion | Ankle dorsi-flexion |
| Session 2 | Elbow extension | Elbow flexion | Ankle dorsi-flexion | Ankle plantar flexion |
| Session 3 | Ankle dorsi-flexion | Ankle plantar flexion | Elbow extension | Elbow flexion |

The active ROM was measured from the neutral position, which is set as 0° . For each movement the muscle stimulated coincides with the muscle from which the sEMG signal is acquired.

In Table 4.3, the specific muscle stimulated/acquired, the stimulation parameters and the electrodes size and type are illustrated for every movements of the protocol.

Table 4.3: Stimulation parameters chosen for every movement performed.

| <i>Movements</i> | <i>Muscle stimulated/ acquired</i> | <i>Pulse width</i> | <i>Frequency</i> | <i>Mode</i> | <i>Inter pulse interval</i> | <i>Electrode size and type</i> |
|-----------------------|--|--------------------|------------------|-------------|---------------------------------|------------------------------------|
| Elbow flexion | biceps brachii | 150 μ s | 40 Hz | triplet | 8 ms | 5x9 cm, rectangular shape |
| Elbow extension | triceps brachii | 200 μ s | 40 Hz | triplet | 8 ms | 5x5 cm, square shape |
| Ankle dorsi-flexion | tibialis anterior | 300 μ s | 40 Hz | triplet | 8 ms | 5x5 cm, square shape |
| Ankle plantar-flexion | gastrocnemius | 350 μ s | 40 Hz | triplet | 8 ms | 5x9 cm, rectangular shape |

The positioning of the acquisition electrodes is displayed in the following figures for the four movements performed. For the upper limbs movements, the reference electrode is placed on the back of the hand. The two active electrodes are placed on the belly of the selected muscle: biceps brachii for elbow flexion and triceps brachii for elbow extension. Instead, for the ankle dorsi-flexion movement the reference electrode is placed on the knee and the two detecting electrodes on the tibialis anterior while in the ankle plantar-flexion the reference is considered as the malleolus while the active electrodes are placed on the gastrocnemius.

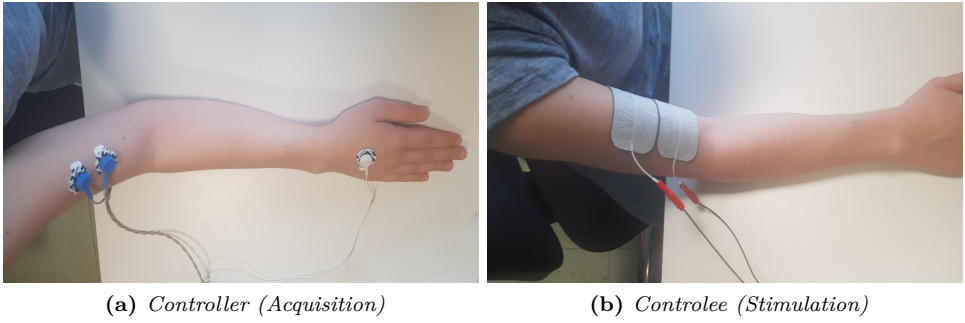


Figure 4.3: Elbow flexion (Biceps brachii)

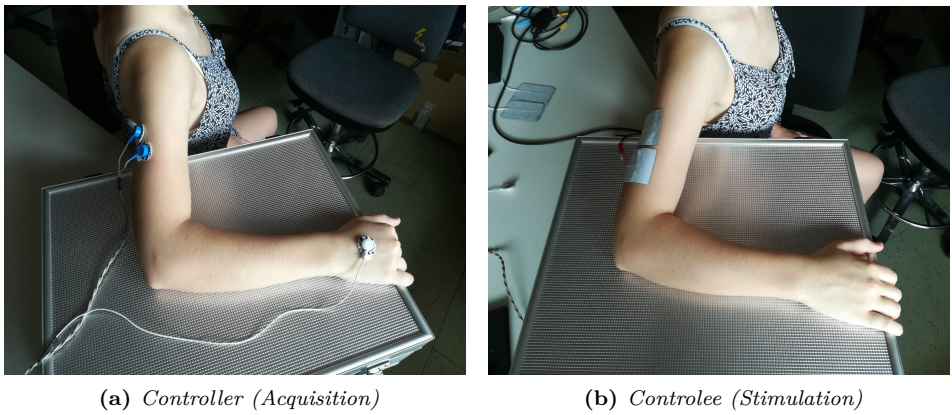


Figure 4.4: Elbow extension (Triceps brachii muscle)

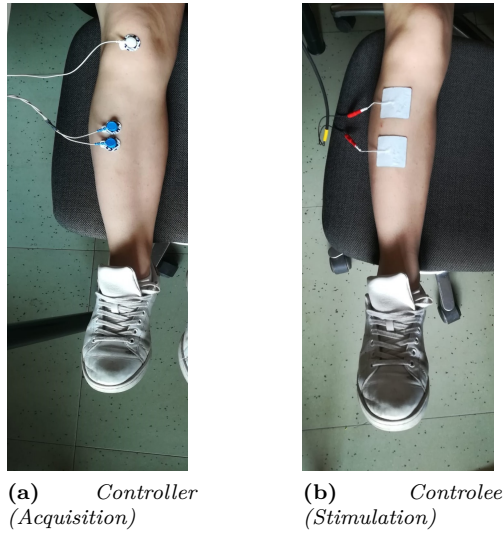


Figure 4.5: Ankle dorsi-flexion (Tibialis anterior)

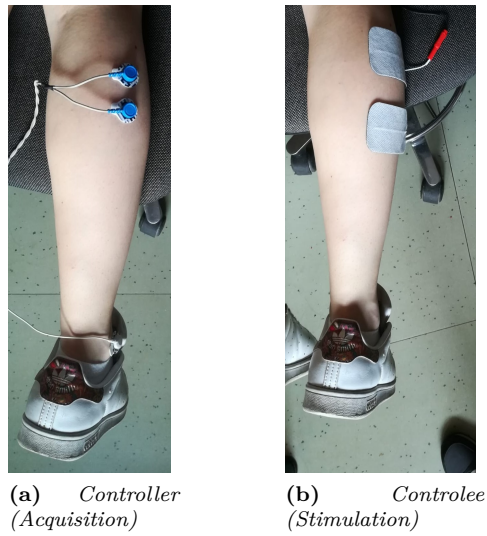


Figure 4.6: Ankle plantar-flexion (Gastrocnemius, lateral head)

4.1.4 Calibration Phase

Before the movement session, an initial FES and TC parameters calibration is implemented as it follows.

sEMG threshold choice

While the therapist is told to be relaxed and motionless, the number of TC events generated is recorded in order to set the most suitable threshold. This process stops and sets automatically the threshold when an event is registered. There is the possibility to choose the initial threshold: the default value is 1.9 V and in any case is advisable not to start from a value lower than 1.85 V to avoid the choice of a too much higher threshold.

ATC parameter setting

Firstly, after the positioning of the acquisition electrodes, the subject acting as a therapist is told to remain motionless in order to set the his proper threshold value as previously explained. Then he performs four movements of the selected limb. The median of the four maximum number of the TC events within the 130 ms time window is recorded and used to determine the number of events generated by the controller needed to deliver a certain current level. Since the number of TC events generated varies from person to person, this setting happens to be important for the overall system performance, since it ensures the correct choice of current pulses number and amplitude.

Maximum AROM measurement

Before the start of any acquisition, the maximum Active Range Of Motion ($AROM_{max}$) of both patient and therapist is measured, asking them to extent the chosen joint as widely as possible from the resting position, in order to normalise the acquired data to this reference value.

Current amplitude setting

The second step is the setting of the maximum current amplitude. This parameter strongly depends on the muscle selected and on the individual subject. Therefore, as suggested by the Hasomed RehaMove[®] manual [31], the stimulation has to be tested before the beginning of the real session for each muscle, stimulating the muscle with a sequence of increasing amplitude pulses and tracking the joint angle in the meanwhile.

The current pulse is delivered for 1.3 s: the amplitude rises gradually until reaching the maximum current value which is held for 520 ms and then decreases to zero.

After a rest period of 3.9 s, the pulse is delivered again with a maximum current value one mA greater than the previous one. The stimulation stops when one of the following conditions occur:

- The patient joint angle exceeds the 70% of its maximum AROM for the upper limbs and the 30% for the lower limbs.
- The maximum stimulation current amplitude reaches 30 mA
- Patient discomfort

The acceptable current intensity is set at a value about 10% higher than the value delivered to the patient just before the stimulation has stopped for the upper limbs and 20% for the lower limbs.

Chapter 5

Data Analysis

5.1 Parameters extraction

A Graphical User Interface was created to display, process and analyse the data acquired (Figure 5.2). The two graphics above in the GUI display respectively the therapist and patient trends while the graphic on the bottom according to the action selected illustrates the stimulation process or the different parameters trends. All the trends showed in the GUI refers to a single repetition of a specific movement.

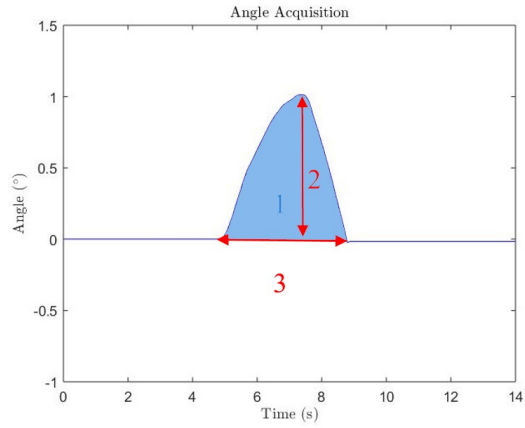
Before analysing the data, the angle signals are processed if needed. In order to remove spikes or oscillations that can be generated by the encoder devices, a low pass filter is applied since these artifacts have a higher frequency than the signal itself. Therefore after analysing the angle Power Density Spectrum (PSD), a Chebychev low pass filter was used having order 5 and with a cut-off frequency of 1.5 Hz. Since the IIR filters are characterised by a nonlinear phase distortion, a zero-phase filtering was performed by means of the "filtfilt" function. This solution provides the best results in removing the angle artifacts in the articular goniometer. Moreover, if necessary, portions of signals that correspond to movements of the patient not related to the stimulation or null therapist stimulations are excluded to allow the calculation of the parameters to be analysed displayed in the table on the bottom portion of the GUI. General information about the patient together with the maximum AROM determined during the calibration phase are displayed in the "General information" panel. The latter value is necessary for the normalisation of the angle trends before the parameters calculation. For this reason the angle values displayed ranges from -1 to 1.

The parameters chosen to evaluate the similarity between the controller and controlled movements are:

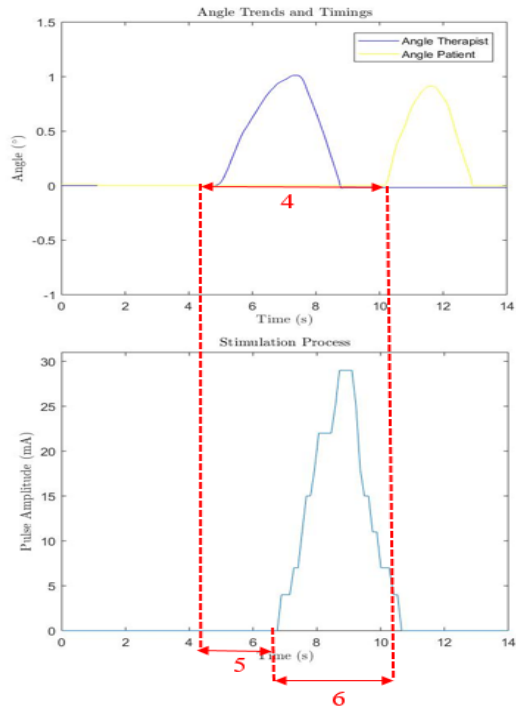
1. Area under the angle trends curve
2. Maximum AROM reached for each movement ($AROM_{max}$)
3. Movement time duration (Δt)
4. Time lapse between the start of the therapist movement and the start of the stimulation (Δt_{th-st})
5. Time lapse between the start of the stimulation and the beginning of the patient movement (Δt_{st-pt})
6. Time lapse between the therapist and patient movement (Δt_{th-pt})
7. Maximum cross-correlation coefficient ($max(\rho_{pt-th})$)

In figure 5.1, the first six parameters are graphically explained.

5.1 – Parameters extraction



(a) 1: area under the curve, 2: $AROM_{max}$, 3: Δt



(b) 4: t_{th-pt} , 5: t_{th-st} , 6: t_{st-pt}

Figure 5.1: Angle features extracted

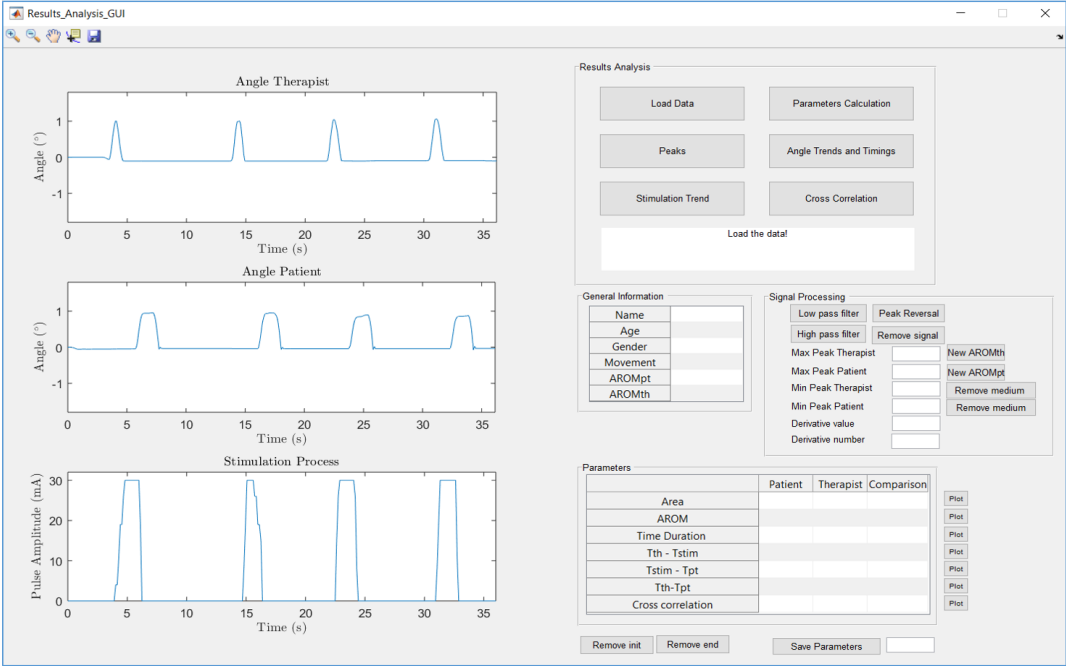


Figure 5.2: Data Analysis GUI

The first five parameters primarily regard the morphology of the signal and should be as similar as possible between controller and controlee. Therefore the difference between the two values is calculated for every cited parameter for each of the ten movements performed during a single repetition. Instead, low timing parameters indicate good real-time performance of the system and high responsiveness of the limb under control to the stimulation. Finally, the cross correlation coefficient is a measure of the degree of similarity between the two movements. It varies from -1 to a maximum value of 1, corresponding to a perfect match between the movements. In order to obtain the value the normalised cross-correlation sequence is computed in Matlab[®] environment as it follows:

$$\hat{R}_{x,y,coeff}(m) = \frac{1}{\sqrt{\hat{R}_{x,x}(0)\hat{R}_{y,y}(0)}}\hat{R}_{x,y}(m)$$

Where m is the lag. The autocorrelation at zero lag equal 1. From this cross correlation sequence the maximum value is considered, whose position corresponds to the lag existing between the two signals.

Each parameter is calculated for each movement and the median value determined

for every repetition (ten movements in total). The result is reported in the last column "Comparison" of the parameters table.

5.2 Fatigue Analysis

In order to assess the possible onset of fatigue, the parameters calculated in the GUI displayed in figure 5.2 are analysed within every session of each of the four movements. The median operator is thus applied to the four movements performed during the three sessions according to the order in which they are performed. In this way a vector of ten values is obtained for each parameters. Afterwards, a comparison is made between the first values of the vector and the last ones so that it is possible to infer the trend of the different parameters from the beginning of the repetition to the end of it. In particular, the median value of the first three movements (p_i) is compared to that of the last three movements (p_f) using the general formula 5.1 for every parameter and obtaining the relative coefficient.

$$c_p = \frac{p_f - p_i}{p_i} 100 \quad (5.1)$$

At this point the minimum, median and maximum values of the coefficients obtained is calculated for every parameters of each of the four selected movements. The results are shown in table 5.1. EF, EE, ADF, APF stand respectively for Elbow Flexion, Elbow Extension, Ankle Dorsi-Flexion, Ankle Plantar-Flexion.

Table 5.1: Parameters analysis within each session

| Parameters % (controller-controllee) | EF | | | EE | | | ADF | | | APF | | |
|---|--------|--------|--------|--------|--------|--------|--------|--------|--------|--------|--------|--------|
| | min | median | max |
| $\max(\rho_{pt-th})$ | -8.72 | -2.43 | 14.52 | -13.05 | 2.86 | 15.38 | -19.70 | 00.49 | 20.60 | -5.90 | 5.37 | 40.62 |
| $Area_{diff}$ | -40.89 | 6.47 | 290.46 | -54.65 | -14.04 | 29.39 | -66.58 | -4.42 | 58.91 | -54.83 | -2.62 | 93.15 |
| Δt_{diff} | -76.73 | 9.16 | 497.88 | -66.63 | -8.03 | 537.88 | -37.03 | -16.80 | 37.50 | -60.87 | -2.21 | 373.98 |
| $AROM_{max_{diff}}$ | -58.67 | 15.78 | 19.53 | -68.99 | 7.75 | 315.64 | -69.67 | 3.66 | 361.05 | -47.60 | 6.87 | 220.85 |
| Δt_{th-pt} | -61.50 | -32.30 | -14.06 | -52.63 | -34.08 | -6.10 | -58.60 | -39.78 | -14.83 | -67.50 | -42.79 | -22.03 |
| Δt_{th-st} | -91.82 | -77.27 | -38.00 | -93.75 | -66.74 | 48.28 | -85.42 | -67.42 | -55.71 | -90.35 | -66.30 | -49.43 |
| Δt_{st-pt} | -39.33 | -1.30 | 19.08 | -11.72 | 0.29 | 43.28 | -35.87 | -3.31 | 7.84 | -41.75 | -4.00 | 7.29 |

From the results in table 5.1, it is possible to notice that the median variation of the maximum cross correlation coefficient ranges from -2.43% (elbow flexion) to 5.37% (ankle plantar-flexion). This means that in the case of elbow flexion $\max(\rho_{pt-th})$ slightly decreases while in the case of ankle dorsi-flexion the value faintly increases. On the contrary as far as $Area_{diff}$, Δt_{diff} , $AROM_{max_{diff}}$ are concerned, a positive value means a worsening of the performance while a negative value an improvement. The median value of all these parameters is globally acceptable: at worst there is a decrease of the performance of 16.8% considering ankle dorsi-flexion. The minimum and maximum values of each parameters are not so relevant considering the great variation of these two outliers in both positive and negative directions. This means

that the overall trending of the parameters within each session does not have a determined direction and therefore, the movement performance is not influenced by the number of repetitions occurring within each session.

As far as the last three timing parameters are concerned (Δt_{th-pt} , Δt_{th-st} , Δt_{st-pt}), the obtained parameter is primarily an indication of the system performance: a positive value represents a decrease of the system performance while a negative value stand for the improvement of the same. It is possible to notice that the timings parameters greatly improves from the beginning to the end of the repetition. The greater contribution is given by Δt_{th-st} , which considerably decreases by the end of the repetition of at least the 66.30% (ankle plantar flexion). Δt_{st-pt} , instead, demonstrates a stable behaviour since its median variation is negligible. Consequently Δt_{st-pt} , the sum of the two previous contribution, considerably improves driven by Δt_{th-st} trend.

5.3 Results

The final obtained results are displayed in Table 5.2. The medium value and the standard deviation of each of the chosen parameters are calculated for every movement performed during the three sessions of all the subjects involved.

Table 5.2: Final results

| <i>Movements</i> | μ_{EF} | σ_{EF} | μ_{EE} | σ_{EE} | μ_{ADF} | σ_{ADF} | μ_{APF} | σ_{APF} |
|-------------------------|------------|---------------|------------|---------------|-------------|----------------|-------------|----------------|
| $max(\rho_{pt-th})$ (%) | 87.18 | 10.47 | 82.68 | 10.80 | 85.04 | 15.69 | 78.88 | 17.04 |
| $Area_{diff}$ (%) | 46.63 | 27.78 | 45.54 | 23.63 | 49.44 | 52.80 | 48.21 | 26.44 |
| Δt_{diff} (%) | 37.40 | 44.58 | 35.13 | 21.00 | 34.58 | 53.56 | 33.56 | 23.32 |
| $AROM_{max_{diff}}$ (%) | 14.33 | 14.02 | 19.68 | 18.63 | 39.10 | 23.55 | 38.45 | 26.82 |
| Δt_{th-pt} (s) | 2.603 | 1.461 | 2.568 | 0.935 | 2.356 | 0.871 | 2.191 | 0.877 |
| Δt_{th-st} (s) | 0.771 | 0.643 | 0.869 | 0.605 | 0.722 | 0.470 | 0.736 | 0.460 |
| Δt_{st-pt} (s) | 1.951 | 1.282 | 1.863 | 0.657 | 1.740 | 0.607 | 1.617 | 0.684 |

The results can be considered satisfying since the medium value of the maximum cross-correlation coefficient is relatively high for every movement: it ranges from 0.79 to a maximum value of 0.87. This means that the system is capable of reproducing the therapist movement with high fidelity. The percentage difference between the area under the angle curves (Δt_{th-st}) is relatively high, since it almost reaches the 50 % in all the movements and the standard deviation is relevant as well. The percentage time duration difference (Δt_{diff}) averages around the 35 % with a standard deviation even higher then the median value while the percentage $AROM_{max_{diff}}$ shows better results for elbow flexion and elbow extension while it greatly worsens for the ankle movements (almost 40 %).

The worse outcomes of $Area_{diff}$ and Δt_{diff} percentages denote the performance of a wider and slower movement by one of the two subjects. In order to enhance this aspect which is difficult or control, the sensibility of the system should be improved so that a larger number of TC event levels and the correspondent current amplitude value could be detected and generated. This fact is widely influenced by the specific physiology of the subject, the response of the individual to the functional electrical stimulation and the training of the therapist.

$AROM_{max_{diff}}$ percentage is related to the factors which have just been cited. Thus, it is also greatly related to the calibration phase, especially the current setting. The percentage added to the 70 % or alternatively the 30 % of the maximum AROM previously measured, might be adjusted in future according to a determined and experimented ratio.

The boxplots relative to each of the four movements are displayed in the following figures.

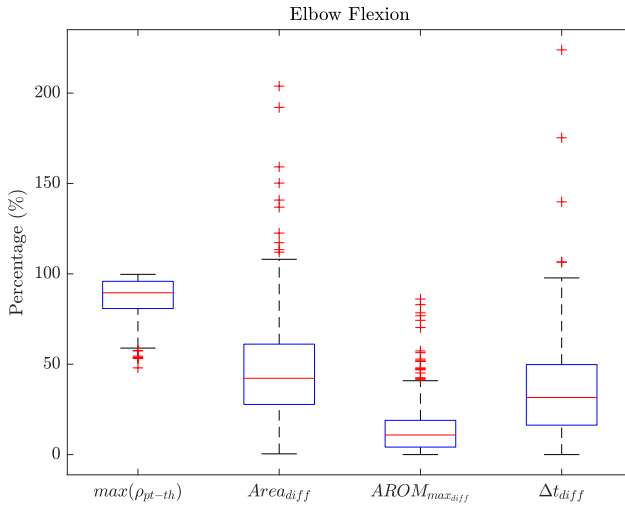


Figure 5.3: Boxplots of the first four parameters for elbow flexion

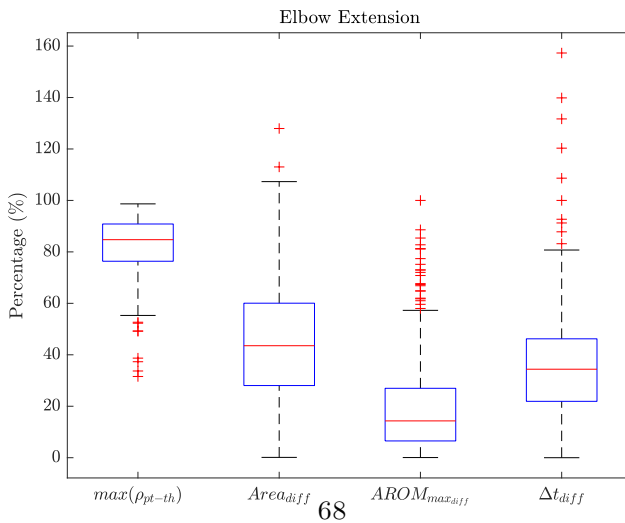


Figure 5.4: Boxplots of the first four parameters for elbow extension

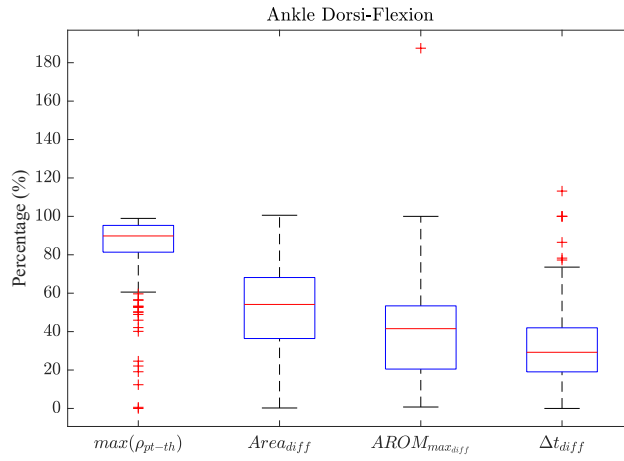


Figure 5.5: Boxplots of the first four parameters for ankle dorsi-flexion

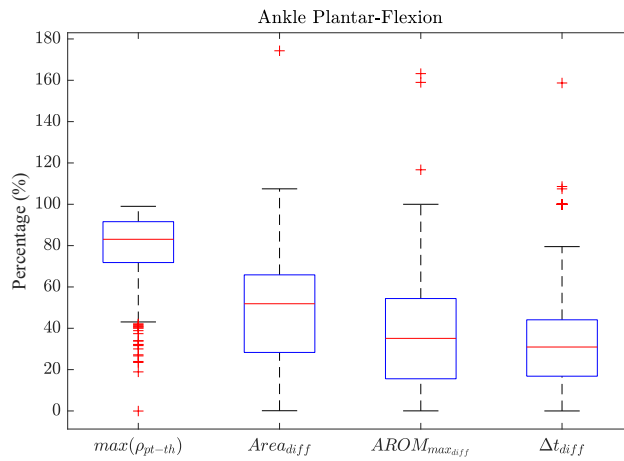


Figure 5.6: Boxplots of the first four parameters for ankle plantar-flexion

5.3.1 System Time Performances

As far as the time features are concerned, it is possible to observe a similar trend between the four movements. The time between the beginning of the therapist movement and the beginning of the patient movement (Δt_{th-pt}) is averagely equal to 2.6 s for elbow flexion, 2.5 s for elbow extension, 2.4 s for ankle dorsi flexion and 1.2 s for ankle plantar flexion. This is the sum of two contributions: the time between the beginning of the therapist movement and the start of the stimulation (Δt_{th-st}) and the start of the stimulation and the beginning of the patient movement (Δt_{st-pt}). The first is the lowest and it includes the receiving of the TC and angle data by the workstation and the elaboration of the most suitable series of current stimuli, while the second represents the largest contribution and it comprises the the time necessary to execute the Simulink[®] RehaStim block, the subsequent arrival of the stimulation data to the stimulator and the patient reaction to the current stimuli. Nevertheless, as it could be highlighted in Table 5.1, Δt_{th-st} decreases noticeably within a single repetition, while Δt_{st-pt} is proved to be more stable. The progressively decreasing of Δt_{th-st} while the stimulation is running is greatly due to the slow response of the system in the first seconds of the Simulink[®] simulation.

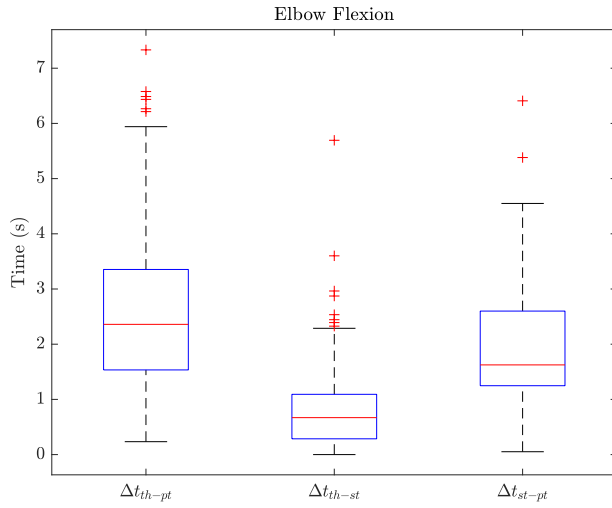


Figure 5.7: Boxplots of the timing parameters for elbow flexion

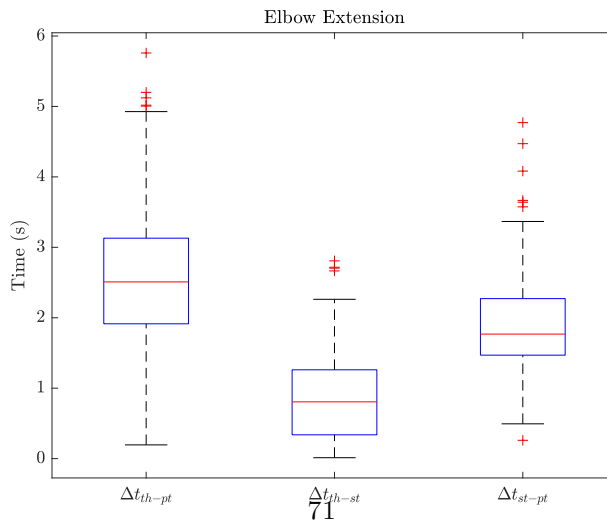


Figure 5.8: Boxplots of the timing parameters for elbow extension

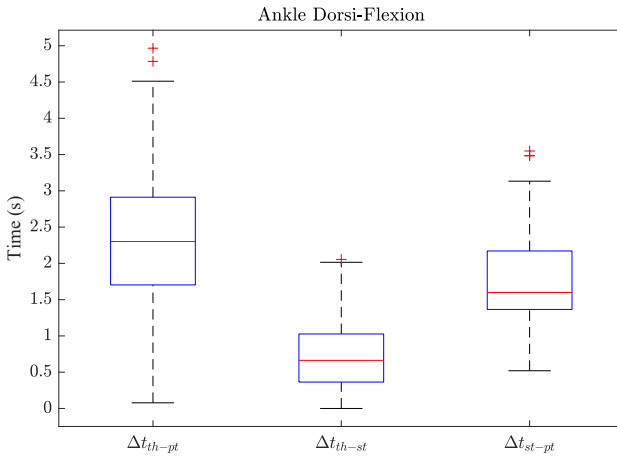


Figure 5.9: Boxplots of the timing parameters for ankle dorsi-flexion

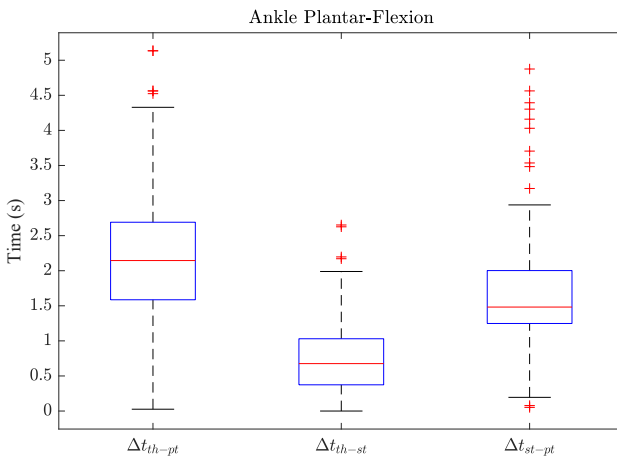


Figure 5.10: Boxplots of the timing parameters for ankle plantar-flexion

Chapter 6

Conclusion

The aim of this thesis project is the improvement and validation of a low power FES rehabilitation system based on the volitional control of the controlee subject movements applying event-driven technique to the sEMG signal acquired from the controller.

The controller contraction information was obtained from the sEMG signal by means of the Average Threshold Crossing technique (ATC) in the acquisition board employed. Afterwards, the information was sent to the workstation via bluetooth communication, and elaborated in order to determine the right parameters of the stimulation to be delivered. In order to assess the degree of similarity between the controller and controlee movements, two articular goniometers were realised using an absolute encoder and an Arduino[®] micro board to acquire the data and send them to the computer via a USB cable. These devices which allowed the tracking of the specific joint angle, were integrated in the acquisition-stimulation system in order to permit the simultaneous acquisition of the TC events and angles data. The actions to be executed were controlled by the user by means of a Matlab[®] GUI which also displayed the real-time plot of the stimulation and angle trends. The data elaboration was conducted in Matlab[®] and Simulink[®] environment while the subsequent delivery of the current pulses were performed by a commercial certificated stimulator.

Before performing the acquisition-stimulation process, a calibration phase was implemented in which the angular data and TC events information was used to set the proper current amplitude suitable for the controlee and the TC events levels for the controller.

After the realisation of the overall system, experimental tests were performed involving nineteen healthy subjects. The experimental protocol which were followed implied the performance ten executions of four types of movements though three sessions.

6.1 Results and future Developments

The system has proved to be capable of reproducing the controller movement in the affected limb of the contolee with a definitively satisfying similarity. As a matter of fact the average cross correlation coefficient in percentage varies from a minimum of 79% (ankle plantar flexion) to a maximum of 87% (elbow flexion). The parameters regarding the area under the angle curve, the maximum active range of motion reached and the duration of the movement are thus not as good as the previous, especially the average $Area_{diff}$ ranges from about 46 % to about 49 % with an high standard deviation value. This result is expected since even though the two movements are recorded by the signal and are highly correlated, it is difficult to reproduce exactly the same movements in terms of duration and extent.

Moreover, it is evident from Δt_{th-pt} , Δt_{th-st} and Δt_{st-pt} that the real-time performance of the system drastically improves during the stimulation. This is due to Simulink[®] whose performances are slower in the first seconds of the simulation. This aspect could be improved optimising the code and alternatively trying to use another environment.

The movement which showed the highest performances is the elbow flexion while the one with the lowest performances is the ankle plantar-flexion. The fact that the reproduction of the ankle plantar flexion is more difficult could due to the complex coordination between several muscles in ankle, foot, and leg not only gastrocnemius. This problem could be solved using several couple of stimulating electrodes having the right size necessary to stimulate the correspondent muscles. Therefore a multi-channel system should be implemented in order to acquire the signals from different muscles and stimulate the correspondent ones in the limb under control. This method should be applied to all the movements performed.

Moreover, in order to improve the mimicking ability, a different calibration phase could improved and a dynamic threshold could be used instead of the fixed one. In this way the selectivity of TC events acquired could be higher to allow a more reliable muscle contraction information. With the number of acquisition obtained, it will be also possible to find a more consistent relationship between the TC events acquired and the corresponding current value.

In the future developments, a system involving also a feedback control on the angular position of both subjects in order to progressively correct the existing error could be a great solution to improve the parameters regarding the area under the angle curve, the maximum active range of motion reached and the duration of the movement.

Nevertheless, the performances are considered good for the overall system and the use of the electrogoniometer has proved to be fundamental not only for the validation of the system, but also during the calibration phase, to set the right

maximum current amplitude value of the patient limb.

Bibliography

- [1] F. M. Trovato, R. Imbesi, N. Conway and P. Castrogiovanni, *Morphological and Functional Aspects of Human Skeletal Muscle*, Journal of Functional Morphology and Kinesiology, no. 1, pp. 289–302, 2016.
- [2] W. R. Frontera and O. J., *Skeletal muscle: A brief review of structure and function*, Calcif Tissue Int, no. 96, pp. 183–195, 2015. doi: 10.1007/s00223-014-9915-y.
- [3] The Editors of Encyclopaedia Britannica *Myofibril*, Encyclopedia Britannica, 2018
- [4] D. Burke, D. C. Gandevia, *Chapter 2 Skeletal muscle: structure and function*, Handbook of Clinical Neurophysiology, Elsevier, vol.2, pp. 7 – 26, 2003, doi: [https://doi.org/10.1016/S1567-4231\(09\)70112-1](https://doi.org/10.1016/S1567-4231(09)70112-1).
- [5] T. Burgoyne, P. K. Luther, *Visualization of cardiac muscle thin filaments and measurement of their lengths by electron tomography*, Cardiovascular Research, April 2008, pp. 707â-712.
- [6] S. Freeman, H. Hamilton, *Biological Science*, 2nd ed., Upper Saddle River, N.J. Pearson Prentice Hall, 2005.
- [7] M. R. Dimitrijevic, J. Faganel, P. C. Sharkey and A. M. Sherwood *Study of sensation and muscle twitch responses to spinal cord stimulation*, International Rehabilitation Medicine, vol. 2, pp. 76-81, doi: 10.3109/09638288009163961.
- [8] C. J. De Luca, A. Adam, R. Wotiz, L. D. Gilmore and S. H. Nawab, *Decomposition of surface EMG signals.*, Journal of neurophysiology, no. 96 3, pp. 1646-57.
- [9] Wikipedia contributors, *Muscle contraction*, Wikipedia, The Free Encyclopedia. Wikipedia, 4 Apr. 2018. Web. 9 May. 2018.
- [10] N. Nazmi, M. A. Abdul Rahman, S. I. Yamamoto, S. A. Ahmad, H. Zamzuri, S. A. Mazlan, *A Review of Classification Techniques of EMG Signals during Isotonic and Isometric Contractions.*, eds. Sensors (Basel, Switzerland), 2016;16(8):1304, doi:10.3390/s16081304.
- [11] R. Merletti, D. Farina, *Surface Electromyography. Physiology, Engineering, and Applications.*

-
- [12] B. S. Rajaratnam, J. CH Goh and V. Prem Kumar, *A Comparison of EMG Signals from Surface and Fine-Wire Electrodes During Shoulder Abduction*, International Journal of Physical Medicine and Rehabilitation, vol. 2, no. 4, OMICS International, doi:10.4172/2329-9096.1000206, 2014.
- [13] M. B. I. Reaz, M. S. Hussain and F. Mohd-Yasin, *Techniques of EMG signal analysis: detection, processing, classification and applications*, Biological Procedures Online, no.8, pp. 11-35, 2006.
- [14] R. H. Chowdhury, M. B. I. Reaz, M. Alauddin Bin Mohd Ali, A. A. A. Bakar, K. Chellappan and T. G. Chang, *Surface Electromyography Signal Processing and Classification Techniques*, Sensors, no. 13, pp. 12431-12466, 2013.
- [15] C. J. De Luca, M. Kuznetsov, L. D. Gilmore, S. H. Roy, *Inter-electrode spacing of surface EMG sensors: Reduction of crosstalk contamination during voluntary contractions*, Journal of Biomechanics (2011), doi:10.1016/j.jbiomech.2011.11.010.
- [16] E. Criswell, *Cram's Introduction to Surface Electromyography*, Second edition, 2011, Jones and Bartlett publishers.
- [17] Carlo J. De Luca, *Surface Electromyography: Detection and Recording*, 2002, Delsys incorporated.
- [18] M. I. Sabri, M. F. Miskon, M. R. Yaacob, *Robust Features Of Surface Electromyography Signal*, IOP Conf. Series: Materials Science and Engineering 53 (2013), doi:10.1088/1757-899X/53/1/012019.
- [19] M. Cifrek, V. Medved, S. Tonkovic, S. Ostojic, *Surface EMG Based Muscle Fatigue Evaluation in Biomechanics*, Clinical Biomechanics, no. 24, pp. 327-340, 2009.
- [20] S. Sapienza, M. Crepaldi, P. Motto Ros, A. Bonanno, and D. Demarchi, *On Integration and Validation of a Very Low Complexity ATC UWB System for Muscle Force Transmission*, IEEE Transactions on Biomedical Circuits and Systems.
- [21] P. Motto Ros, M. Paleari, N. o Celadon, A. Sanginario, A. Bonanno, M. Crepaldi, P. Ariano and D. Demarchi, *A Wireless Address-Event Representation System for ATC-Based Multi-Channel Force Wireless Transmission*.
- [22] K. Takeda, G. Tanino, H. Miyasaka, *Review of devices used in neuromuscular electrical stimulation for stroke rehabilitation*, Medical Devices (Auckland, NZ), 2017;10:207-213, doi:10.2147/MDER.S123464.
- [23] National Clinical Guideline Centre, *Stroke Rehabilitation: Long term rehabilitation after stroke*, Clinical guideline 162, Methods, evidence and recommendations, 29 May 2013
- [24] Functional electrical stimulation (FES). (n.d.). Retrieved from <https://www.mstrust.org.uk/a-z/functional-electrical-stimulation-fes>
- [25] HASOMED RehaMove Catalogue, HASOMED GmbH, Germany, 2016
- [26] ROM (range of motion) information. (n.d.). Retrieved

- from <https://bonesmart.org/forum/threads/rom-range-of-motion-information.3730/>
- [27] Capacitive Absolute Encoders AMT20 Series. (n.d.). Retrieved from <https://www.cui.com/product-spotlight/capacitive-absolute-encoders-amt20-series>
- [28] Collins, D. (2015, October 29). FAQ: What are capacitive encoders and where are they suitable? Retrieved from <https://www.motioncontroltips.com/faq-what-are-capacitive-encoders-and-where-are-they-suitable/>
- [29] Y. X. Zhou, H. P. Wang, X. P. Cao, Z. Y. Bi, Y. J. Gao, X. B. Chen X. Y. Lu and Z. G. Wang, *Electromyographic Bridge—A Multi-Movement Volitional Control Method for Functional Electrical Stimulation: Prototype System Design and Experimental Validation*, Engineering in Medicine and Biology Society (EMBC), 2017 39th Annual International Conference of the IEEE, doi: 10.1109/EMBC.2017.8036798.
- [30] Operational Manual RehaStim2, RehaMove2, version 1.4 / 2012-09 HASOMED GmbH
- [31] What is Motor Threshold (MT). (n.d.). Retrieved from <https://www.igi-global.com/dictionary/motor-threshold-mt/19274>
- [32] Wikipedia contributors, *Serial Peripheral Interface Bus*, Wikipedia, The Free Encyclopedia. Wikipedia, 12 May. 2018. Web. 22 May. 2018.
- [33] AMT20 Series 28 mm, Capacitive Modular Encoder datasheet.
- [34] Kendallâ€™ ECG Electrodes Product Data Sheet ArboTM H124SG Ref. Code: 31.1245.21
- [35] B. Kuberski, *ScienceMode2, RehaStim2 Stimulation Device, Description and Protocol*, 12 December 2012, Hasomed GmbH.
- [36] Chapter 5-Webster Biopotential Electrodes. (n.d.). Retrieved from <https://slideplayer.com/slide/3452273/12/>
- [37] Monopolar vs. Bipolar EMG Readings. (2014, September 18). Retrieved from <https://www.nrsign.com/monopolar-vs-bipolar-emg-readings/>
- [38] M. Z. Jamal, *Signal Acquisition Using Surface EMG and Circuit Design Considerations for Robotic Prosthesis*, Computational Intelligence in Electromyography Analysis Ganesh R. Naik, IntechOpen, DOI: 10.5772/52556
- [39] S. Bianca, *Design and development of a low-power wearable device for the acquisition of surface electromyography (sEMG) signals with average threshold crossing (ATC)*, Master's thesis, Politecnico di Torino, 2016.
- [40] E. Cordedda, *Riconoscimento real time di gesti applicato a segnali EMG superficiali basato su ATC*, Master's thesis, Politecnico di Torino, 2016.
- [41] J. Iqbal, U. Izhar, U. S. Khan, N. Rashid *Optimized circuit for EMG signal processing*, 2012 International Conference on Robotics and Artificial Intelligence, ICRAI 2012. 208-213. 10.1109/ICRAI.2012.6413390.
- [42] G. Del Luca, *Fundamental Concepts in EMG Signal Acquisition*, DelSys Inc, 2001, Rev.2.1, March 2003.

- [43] I. Furfaro, *Integration and validation of average threshold crossing (ATC) applied to surface electromyography (semg)*, Master's thesis, Politecnico di Torino, 2015.
- [44] E. Da Luz dos Santos, M. C. Gelain, E. Krueger, G. Nunes Nogueira-Neto, P. Nohama, *Artificial motor control for electrically stimulated upper limbs of plegic or parietic people*, Research on Biomedical Engineering, Vol. 32, No. 2, pp. 199-211, 2016, doi: <http://dx.doi.org/10.1590/2446-4740.03415>.
- [45] Y. Hara, *Rehabilitation with Functional Electrical Stimulation in Stroke Patients*, International Journal of Physical Medicine Rehabilitation, Int J Phys Med Rehabil 1: 147. doi:10.4172/2329-9096.1000147.
- [46] K. Shima K. Shimatani, *A New Approach to Direct Rehabilitation Based on Functional Electrical Stimulation and EMG Classification*, International Symposium on Micro-NanoMechatronics and Human Science (MHS), 28-30 Nov. 2016, doi: 10.1109/MHS.2016.7824200.
- [47] Triceps. (n.d.). Retrieved from <http://www.ganfyd.org/index.php?title=Triceps>
- [48] F. Rossi, *Low Power System for Event-Driven Control of Functional Electrical Stimulation*, Master's thesis, Politecnico di Torino, 2017.